NASA TM-85027

NASA-TM-85027 19830019657

A Reproduced Copy

OF

NASA TM- 85027

Reproduced for NASA

by the

NASA Scientific and Technical Information Facility

LIBRARY COPY

1984

LANGLEY RESEARCH CENTER
LIBRARY, NASA
HAMPTON, VIRGINIA

FFNo 672 Aug 65

(NASA-TM-85027) NASA/GODDARD SPACE FLIGHT CENTER CONTRIBUTIONS TO THE WORKSHOP ON POSITRON-ELECTRON PAIRS IN ASTROPHYSICS (NASA) 62 p HC A04/MF A01 CSCL 03B
N83-27928
THRU
N83-27937
Unclas
G3/88 11793

NASA

Technical Memorandum 85027

NASA/Goddard Space Flight Center Contributions to the Workshop

on

POSITRON-ELECTRON PAIRS IN ASTROPHYSICS

M.L. Burns, T.L. Cline, J.K. Daugherty
R.J. Drachman, N. Gehrels, A.K. Harding
D. Kazanas, R.E. Lingenfelter, J.M. McKinley
W.S. Paciesas, R. Ramaty, R.A. Shafer
B.J. Teegarden, J. Tueller

JUN 1983
RECEIVED
NASA STI FACILITY
ACCESS DEPT.

MARCH 1983

National Aeronautics and
Space Administration

Goddard Space Flight Center
Greenbelt, Maryland 20771

N83-27928

NASA/GODDARD SPACE FLIGHT CENTER
Contributions to the Workshop on

POSITRON-ELECTRON PAIRS IN ASTROPHYSICS

Contents

"An Electron-Positron Jet Model for the Galactic Center", M. L. Burns. . .1

"Comparison of Photon-Photon and Photon-Magnetic Field Pair Production Rates", M. L. Burns and A. K. Harding. 7

"Pair Production and Annihilation in Strong Magnetic Fields", J. K. Daugherty and A. K. Harding. 13

"Low-Temperature Positron Annihilation", R. J. Drachman. 27

"Upper Limits to the Annihilation Radiation Luminosity of Centaurus A", N. Gehrels, T. L. Cline, W. S. Paciesas, B. J. Teegarden and J. Tueller. 39

"Pair Production Near Threshold in Pulsar Magnetic Fields", A. K. Harding and J. K. Daugherty. 45

"e^+-e^- Annihilation and the Cosmic X-Ray Background", D. Kazanas and R. A. Shafer. 51

"The Origin of the Galactic Center Annihilation Radiation", R. E. Lingenfelter and R. Ramaty. 57

"Criteria for GRASAR Action in Astrophysical Sources", J. M. McKinley and R. Ramaty. 63

N83
27929

UNCLAS

N83 27929

D1

ORIGINAL PAGE IS
OF POOR QUALITY

AN ELECTRON-POSITRON JET MODEL FOR THE GALACTIC CENTER

M. L. BURNS
NASA/GODDARD SPACE FLIGHT CENTER
GREENBELT, MD 20771
and
DEPARTMENT OF PHYSICS and ASTRONOMY
UNIVERSITY OF MARYLAND
COLLEGE PARK, MD 20742

ABSTRACT

High energy observations of the galactic center on the subparsec scale seem to be consistent with electron-positron production in the form of relativistic jets. These jets could be produced by a $\sim 10^6$ $M_\odot$ black hole dynamo transporting pairs away from the massive core. An electromagnetic cascade shower would develop first from ambient soft photons and then non-linearly; the shower using itself as a scattering medium. This is suited to producing, cooling and transporting pairs to the observed annihilation region. It is possible the center of our galaxy is a miniature version of more powerful active galactic nuclei that exhibit jet activity.

OBSERVATIONS

Interesting activity from the heart of our galaxy has been observed over the past few years. Specifically, a luminous line at 0.511 MeV has been detected which is suprisingly narrow and variable.[1] In addition, the region from which this line emanates coincides with a small and less luminous radio source.[2] A short list of these observations follows:

1. A 10^6 $M_\odot$ object at the galactic center could be inferred from the widths of Neon lines in HII clouds orbiting the central region.[3]

2. Luminosities are: 10^{38} erg/s in continuum gamma rays[4]; 10^{37} erg/s in 0.511 MeV line[1]; 10^{37} erg/s in hard X-rays[4]; 10^{35} erg/s in soft X-rays[4]; 10^{40} erg/s in UV[3]; 10^{41} erg/s in IR[5] and 10^{33} erg/s in radio.[2]

3. The 0.511 MeV line is variable on approximately a six month time scale.[1]

4. The line was measured at (510.9 ± 0.25)keV.[6]

5. A compact radio source is resolved to less than 10^{15} cm in size.[2]

ORIGINAL PAGE IS
OF POOR QUALITY

CONSTRAINTS

Two important constraints come from the line. First, the six month variability constrains the size of the region producing the line to be less than or equal to six light months in extent. It is possible the radio source is an even more stringent constraint on size. Secondly, the annihilation region must be separated from any massive object by at least $\sim 10^3[2GM/c^2]$($\sim 10^{15}$ cm for a 10^6 $M_\odot$ black hole) so that the line will not be gravitationally redshifted out of the observed narrow energy range. Since the compact radio object exhibits spectral properties similiar to the cores of active galaxies, this coupled with the observed higher energy phenomena leads one to consider scaled down versions of power sources for active galaxies.

MODEL

A black hole dynamo producing relativistic e^+-e^- jets of the type proposed by Lovelace[7,8] for double radio sources will be considered here. Other beam models have been considered by Brown[9], Blandford[10] and Novikov.[11] Relativistic electron-positron jets seem necessary because:

1. A line is observed at 0.511 MeV implying annihilation of e^+-e^- pairs.

2. A jet would beam pairs into an annihilation region far enough from the massive engine to be consistent with the width of the line and bypasses the problem of producing pairs to close to the engine.

3. The natural propagation of a relativistic jet would convert kinetic energy into rest mass of pairs thereby simultaneously producing them and transporting them out.

4. Relativistic beaming maintains a confined interaction region in which high energy particles can interact with one another.

A dynamo, possibly powering a quasar, produces a luminosity, $L \sim 10^{44}(M/10^8 M_\odot)^2(B/10^3 G)^2$ erg/s.[8] For the galactic center a $\sim 10^6$ $M_\odot$ black hole and line luminosity of $\sim 10^{37}$ erg/s results in a dynamo magnetic field of $\sim$ 30 Gauss. Using this field, an accelerating potential can be calculated. It is $V \sim 10^{19}(M/10^8 M_\odot)(B/10^3 G)$ V $\sim 10^{15}$ V. The resulting electron flow from the engine is $I \sim 10^{37}(M/10^8 M_\odot)(B/10^3 G)$ e/s $\sim 10^{34}$ e/s. These collimated fast electrons will then interact with the dominant scattering background. This background initially appears to be the infrared radiation however the majority of interstellar dust that could be correlated with IR is believed to be outside of the central parsec[5] thereby making it impossible for electrons to cool against it. However $\sim 10^{40}$ erg/s in ionizing UV must be produced from a 3.2×10^4 °K region within the central parsec to be consistent with HII

ORIGINAL PAGE IS
OF POOR QUALITY

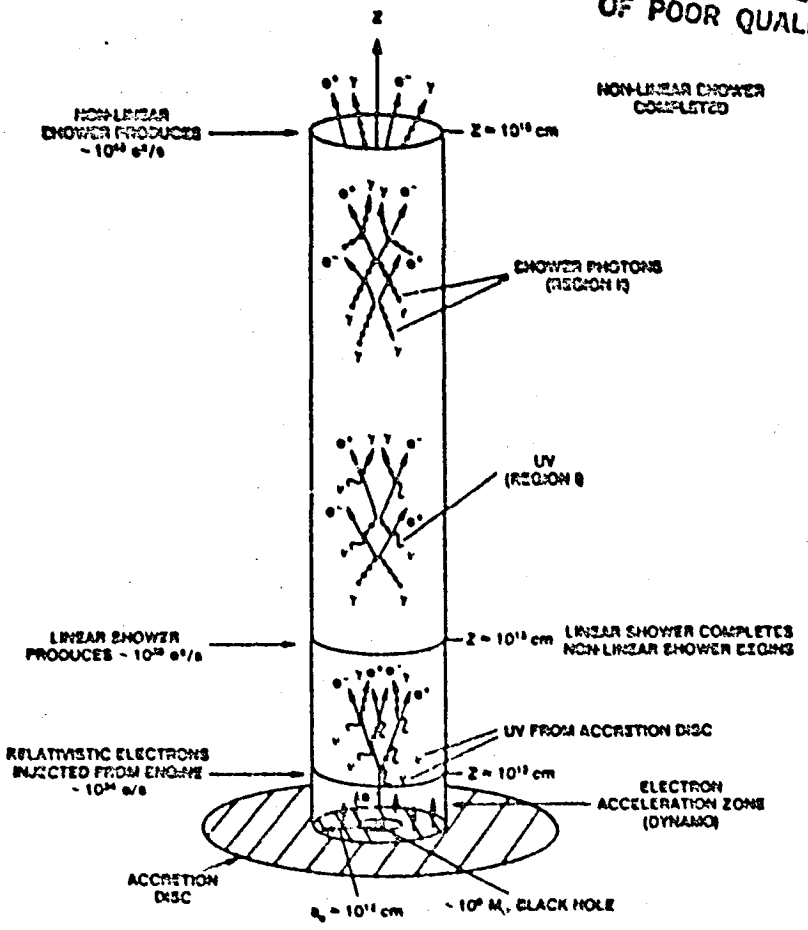

Figure 1. Schematic of Electron-Positron Jet at Galactic Center

observations.[3] An accretion disc emitting UV at a density of $\sim 10^{15}$ cm^{-3} from $\sim 10^{26}$ cm^2 could supply a cooling medium for fast electrons, this setting a cross-sectional radius of $a_0 \sim 10^{12}$ cm for the jet (Figure 1). Since the compact radio source is smaller than $\sim 10^{15}$ cm, it would seem the bulk of fast particles are not propagated past that distance. The radio therefore sets a length of the jet at $\ell \sim 10^{15}$ cm. Knowledge of the observed 0.511 MeV line flux and necessary photon reaction rate quite independently enables one to constraint the dimensions of the source.[12] For beam geometry it is found the length and cross-sectional radius must be related by $a_0^2/\ell \sim 10^9$ cm for photon-photon interactions to occur. The UV-radio estimates of the jet dimensions are then consistent with constraints from photon-photon reactions.

ORIGINAL PAGE IS
OF POOR QUALITY

CASCADE SHOWER

In the vinicity of the dynamo ($\sim 10^{12}$ cm) an electromagnetic cascade will develop by the interaction of collimated fast electrons with UV. Pairs will be produced, in a linear fashion, as kinetic energy is degraded from $\sim 10^{15}$ eV to $\sim 10^{11}$ eV, the pair production threshold. At a distance of $\sim 10^{13}$ cm, pair production from the UV will cease because the UV density is decreasing with increasing distance. The yield of pairs , $f_{\pm}$, can be calculated from coupled relativistic Boltzmann transport equations.[13] The spectrum behaves roughly as a power law,

$$\text{Linear:} \quad f_{\pm}(z,E) \sim e^{\tau(z)} \left(\frac{E_o}{E}\right)^{s+1} \qquad (1)$$

Here z is the distance into the shower from the injection point at $\sim 10^{12}$ cm, E_o is the primary energy from the engine and E is the energy. The optical depth of the shower particles to UV is

$$\tau(z) = 10 \left[1-\left(\frac{a_o}{z}\right)^3\right] \qquad (2)$$

where $a_o \approx 10^{12}$ cm is the engine radius. The flux of shower particles has then increased from $\sim 10^{34}$ e/s injected by the engine to $\sim 10^{38}$ $e^{\pm}$/s as a result of linear cascade action.

Although pair production from the UV has ceased, continued cooling of pairs from the UV (Figure 1, Region I) will produce hard photons energetic enough to sustain pair production in a non-linear fashion. The non-linear shower proceeds as follows. Hard photons produced by inverse Compton of the UV will pair produce. Those pairs then cool by inverse Compton, producing more hard photons which further pair produce and so on. However, since the UV density is dropping with distance and the shower population is growing, at some point the soft photons in the shower will dominate the UV (Figure 1, Region II). The cascade then proceeds using soft photons in the shower as a medium until pair production threshold is reached. The end products are then cooled pairs and hard X-rays, below threshold, of comparable luminosities ($\sim 10^{37}$ erg/s). The yield of pairs, $f_{\pm}$, can be calculated for the non-linear shower from coupled transport equations.[14] The simpler solutions yield power laws of the form

$$\text{Non-linear:} \quad f_{\pm}(z,E) \sim \left[1 - \lambda \left(\frac{z}{z_o} - 1\right)\right]^{-1} \left(\frac{\epsilon_o}{E}\right)^{\bar{s}+1} \qquad (3)$$

Here z is the distance into the shower, $z_o \approx 10^{13}$ cm is the starting position of the non-linear shower and ϵ_o, the primary energy, is the typical energy emerging from the linear shower. The spatial dependence exhibits the large non-linear growth of the pairs

ORIGINAL PAGE IS
OF POOR QUALITY

possible at $z/z_0 \approx 1+\lambda^{-1}$. Depending on the value of λ, the growth may be explosive ($\lambda >> 1$) or adiabatic ($\lambda << 1$). This parameter estimated for the galactic center would imply a slow buildup of pairs. An interesting aside is the possible application of the explosive solutions to gamma ray bursts. In any case, the completed non-linear shower has now increased the particle flux from $\sim 10^{38}$ e±/s to $\sim 10^{43}$ e±/s at a distance of $\sim 10^{15}$ cm.

Electrons and positrons will now drift into a region, possibly an HII cloud[12], and annihilate to form the 0.511 MeV line. Pairs are now past the point where the black hole could gravitationally redshift the line out of the observed range and are also cool enough not to significantly contribute to the compact radio source past $\sim 10^{15}$ cm. It can now been seen that variability in the 0.511 line could be caused by variability in the dynamo itself. For instance pinching of the beam could cause the observed changes of line intensity and would predict correlated hard X-ray and 0.511 MeV line variability.

The density of pairs leaving the beam is $\sim 10^7$ cm^{-3}. If an HII cloud is to act as a beam bag and subsequent annihilation region, the energy density of the beam should be comparable to the energy density of the cloud. If the pairs have energies of 1-10 MeV, a calculated cloud density is $n_{cloud} \approx \gamma m_e n_+/m_p \approx 10^5$ cm^{-3}. This is consistent with H_2CO(formaldehyde) and NH_3(ammonia) observations.[15]

SUMMARY

The model developed here supplies an annihilation region with the correct flux of relatively cool pairs at the proper distance from the engine. Hard X-rays would be produced with comparable luminosity to the 0.511 MeV line and their variabilities would be directly correlated. An HII cloud appears to be consistent with stopping cooled pairs from the jet. The proposed jet at the galactic center deposits more of its energy in the 0.511 MeV line as opposed to the radio unlike its more powerful counterpart in an active galaxy. This could be telling us the position of the acceleration point with respect to the central material. For an active galaxy acceleration occurs further out; the kinetic energy feeding a radio source. For an object like the galactic center, acceleration occurs closer in; the kinetic energy converting to rest mass which feeds an annihilation line.

ACKNOWLEDGEMENTS

The author would like to thank R. Lovelace, D. Leiter, R. Ramaty, R. Lingenfelter and the High Energy Astrophysics Theory Group at Goddard for useful discussions.

ORIGINAL PAGE IS
OF POOR QUALITY

REFERENCES

1. M. Leventhal and C. J. MacCallum, The Galactic Center, AIP Conf. Proc. 83,132(1982).
2. K. Y. Lo, The Galactic Center, AIP Conf. Proc. 83,1(1982).
3. J. H. Lacy, The Galactic Center, AIP Conf. Proc. 83,53(1982).
4. J. L. Matteson, The Galactic Center, AIP Conf. Proc. 83,109(1982).
5. I. Gatley, The Galactic Center, AIP Conf. Proc. 83,25(1982).
6. A. S. Jacobson, The Galactic Center, AIP Conf. Proc. 83,123(1982).
7. R. V. E. Lovelace,Nature,262,649(1976).
8. R. V. E. Lovelace, J. MacAuslan and M. Burns, Particle Acceleration Mechanisms in Astrophysics, AIP Conf. Proc. 56,399(1979).
9. Robert L. Brown, Ap. J.,262,110(1982).
10. R. D. Blandford, The Galactic Center, AIP Conf. Proc. 83,177(1982).
11. I. D. Novikov, these proceedings.
12. R. E. Lingenfelter and R. Ramaty, The Galactic Center, AIP Conf. Proc. 83,148(1982).
13. M. L. Burns and R. V. E. Lovelace,Ap. J.,262,87(1982).
14. M. L. Burns in preparation.
15. R. Gusten, The Galactic Center, AIP Conf. Proc. 83,9(1982).

PAGE _____ INTENTIONALLY BLANK

N83
27930

UNCLAS

ORIGINAL PAGE IS
OF POOR QUALITY

N83 27930

D2

COMPARISON OF PHOTON-PHOTON AND PHOTON-MAGNETIC FIELD PAIR PRODUCTION RATES

M. L. Burns* and A. K. Harding
NASA/Goddard Space Flight Center, Greenbelt MD 20771

ABSTRACT

Neutron stars have been proposed as the site of gamma-ray burst activity and the copious supply of MeV photons admits the possibility of electron-positron pair production. If the neutron star magnetic field is sufficiently intense ($> 10^{12}$ G), both photon-photon (2γ) and photon-magnetic field (1γ) pair production should be important mechanisms. Rates for the two processes have been calculated using a Maxwellian distribution for the photons. The ratio of 1γ to 2γ pair production rates has been obtained as a function of photon temperature and magnetic field strength.

INTRODUCTION

Observations of the spectra of gamma-ray bursts indicate the presence of significant numbers of high energy photons in the Mev range. Some spectra have features at energies between 350 and 450 keV[1], which have been interpreted as red-shifted annihilation lines. The amount of the shift (~10%) is the gravitational red-shift expected from the potential well of a neutron star. In addition, absorption features have been observed in many of the spectra in the region 20 - 60 keV, which if interpreted as cyclotron absorption, indicate magnetic fields of order 10^{12} G. The evidence seems to suggest that the emitting regions of these sources are near the surfaces of strongly magnetized neutron stars.

If this is the case, then one-photon as well as two-photon processes might be expected to contribute to the production of pairs in gamma-ray burst sources. One-photon pair production, a first order process which is forbidden in free space, is allowed in the presence of a magnetic field. If the photons have a thermal distribution, then significant pair production rates will occur when $(kT/mc^2)(B/B_{cr}) \gtrsim 0.1$.

ONE-PHOTON PAIR PRODUCTION RATE

We first calculate the rate of 1γ pair production in a hot photon gas where the photons have a Maxwellian distribution. The rate for a single photon with energy E propagating at an angle θ to a constant, homogeneous magnetic field of strength B is[2]:

*Also University of Maryland, College Park, MD 20742.

ORIGINAL PAGE IS
OF POOR QUALITY

$$r_{\gamma B} \sim \frac{1}{2} \frac{c\alpha}{\lambda\!\!\!^{-}} \frac{B\sin\theta}{B_{cr}} T(\chi), \tag{1}$$

$$T(\chi) = 4.74\, \chi^{-1/3}\, Ai^2\, (\chi^{-2/3}) \tag{1a}$$

$$\sim 0.46 \exp\left[-4/3\chi\right], \quad \chi \ll 1 \tag{1b}$$

$$\sim 0.60\, \chi^{-1/3}, \quad \chi \gg 1 \tag{1c}$$

where $\chi \equiv \left(\frac{E}{2mc^2}\right)\left(\frac{B}{B_{cr}}\right) \sin\theta$, $B_{cr} = 4.414 \times 10^{13}$G, and Ai is the Airy function.

These are the asymptotic expressions in the limit where the quantum numbers of the magnetic field pair states are large. We will discuss the region of validity of this expression below. The pair production rate for a distribution of photons, $\Phi(E,T)$, will be

$$R_{\gamma B}(B,T) = 2\pi \int_0^{\pi} \sin\theta d\theta \int_{E_{min}}^{\infty} dE\, \Phi(E,T)\, r_{\gamma B}(E,B,\theta)\, s^{-1} \tag{2}$$

where $E_{min} = 2mc^2/\sin\theta$ is the threshold photon energy. We take a Maxwellian distribution for the photons, normalized to constant photon number density:

$$\Phi(E,T) = \frac{E^2}{2(kT)^3} \exp(-E/kT) \tag{3}$$

If we make the further approximations, $\chi \ll 1$ and $E \gg 2mc^2$ then an analytic expression can be obtained for the pair production rate. The E integration of Eqn (2) can be performed by the method of steepest descents. The integrand has a saddle point at $E_o = mc^2 [(8/3)(kT/mc^2)(B_{cr}/B \sin\theta)]^{1/2}$, about which the major contribution to the integral is located. The θ integral can then be performed by noting that the integrand peaks very sharply around $\sin\theta = 1$. The result for the photon distribution of Eqn (3) is

$$R_{\gamma B}(B,T) = 7.92 \times 10^{19} \frac{mc^2}{kT} \exp\left[-2\left(\frac{8}{3}\frac{mc^2}{kT}\frac{B_{cr}}{B}\right)^{1/2}\right] s^{-1} \tag{4}$$

where the above approximations translate into the regions of validity for this expression:

$$\left(\frac{kT}{mc^2}\frac{B}{B_{cr}}\right)^{1/2} \ll 1, \qquad \frac{kT}{mc^2} > \frac{3}{2}\frac{B}{B_{cr}}. \tag{5}$$

It is evident that Eqn (4) is not valid for magnetic fields approaching the critical value or at low temperatures, where most of the photons have energies near threshold.

ORIGINAL PAGE IS
OF POOR QUALITY

To obtain the behavior of the one-photon pair production rate in the full region of interest, we have numerically integrated Eqn. (2), taking into account the photon energy threshold and the full asymptotic rate [Eqns. (1), (1a)]. Figure 1 shows this rate per photon as a function of kT and B. Due to the exponential behavior of Eqn. (1b) at low photon energies, the calculated rate is a very sensitive function of T and B at low temperatures. At temperatures below $kT = mc^2$, slight variations in B can change the rate by many orders of magnitude.

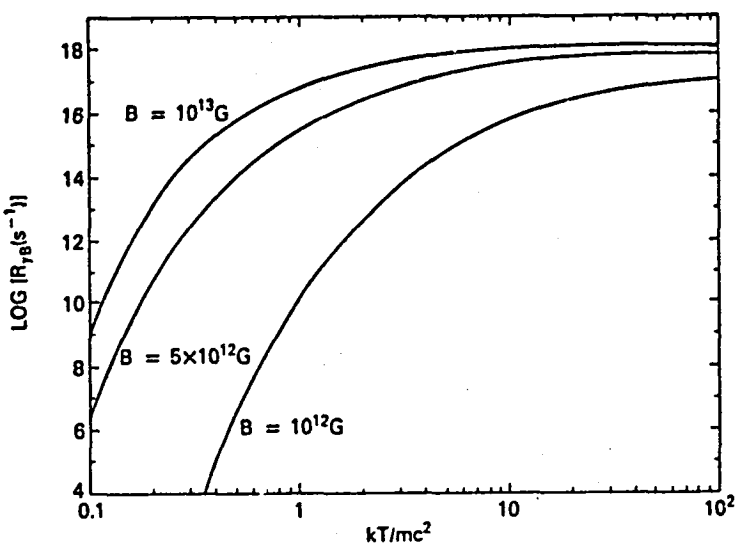

Fig. 1. 1γ pair production rate per photon versus kT/mc^2 for different magnetic field strengths.

RATIO OF ONE-PHOTON TO TWO-PHOTON PAIR PRODUCTION

The pair production rate via the two-photon process can be calculated for the same photon gas with a Maxwellian distribution of energies in order to directly compare the one-photon to the two-photon rate. In the case of photon-photon pair production, we must integrate the cross-section and the photon distribution over both photon energies, E and E', and the angle, θ, between their propagation vectors (see eg. Ref. 3):

$$R_{\gamma\gamma}(T) = \frac{1}{2}\, 2\pi c \int_0^{\pi} d\theta \, \sin\theta \, (1-\cos\theta) \int_0^{\infty} dE \int_{E_{min}(E,\theta)}^{\infty} dE'$$

$$\Phi(E,T)\, \Phi(E',T)\, \sigma(E,E',\theta)\ s^{-1} cm^3 \qquad (6)$$

where $E_{min}(E,\theta) = 2\, m^2c^4/E(1-\cos\theta)$

ORIGINAL PAGE IS
OF POOR QUALITY

The cross-section is[4]

$$\sigma(E,E',\theta) = \frac{3}{2}\,\sigma_T\,\sigma(\tau) \tag{7}$$

where

$$\sigma(\tau) = \frac{1}{\tau^3}\left\{(\tau^2 + 4\tau - 8)\,\ln\left[\frac{\sqrt{\tau}+\sqrt{\tau-4}}{\sqrt{\tau}-\sqrt{\tau-4}}\right] - (\tau+4)\sqrt{\tau(\tau-4)}\right\}$$

and $\tau(E,E',\theta) = \frac{2EE'}{m^2c^4}(1-\cos\theta)$.

and the photon distribution is given by Eqn (3). Numerical integration of Eqn (6) then enables us to evaluate the relative importance of the one- and two-photon processes. Figure 2 shows the ratio of the one-photon to the two-photon pair production rates as a function of kT. The vertical scale plots, on the left hand side, the photon density (which is kept constant with T) for which the two rates are equal and on the right hand side, the actual ratio of the rates at a fixed density of 10^{25} cm^{-3}. Also plotted is the blackbody photon density n_{BB}(dashed line) which is the maximum photon density achievable at a given temperature. At temperatures below $kT = mc^2$, which are the temperatures of interest for gamma-ray burst sources, a change in the magnetic field of one order of magnitude corresponds to many orders of magnitude in the ratio of the two rates. From Figure 2, one can obtain, for a given photon density and magnetic field strength, the temperature at which either process dominates. For example, for a photon density $n = 10^{25}$ cm^{-3} and $B = 10^{12}$ G, the one-photon process dominates over the two-photon process at $kT > mc^2$. For $B > 4 \times 10^{12}$ G, one-photon pair production is the dominant process at all temperatures.

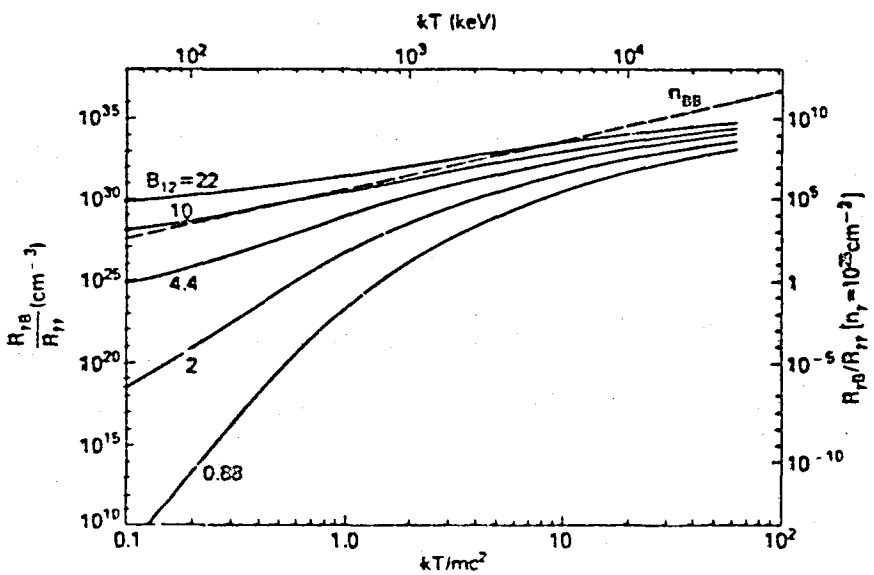

Fig. 2. Ratio of 1γ to 2γ pair production rates for Maxwellian photon distributions at temperature kT. Curves are labeled with values of the magnetic field in units of 10^{12} G.

ORIGINAL PAGE IS
OF POOR QUALITY

DISCUSSION

In a magnetic field, electron and positron energies perpendicular to the field are quantized, with the energy separation between the levels increasing with field strength. When the photon energies are not large compared to the spacing between these Landau states, the pair production rates are significantly influenced by quantum effects. In the preceeding calculations, we have neglected the effect of the discrete e^+e^- states on the pair production rates. In the case of the one-photon rate, quantum effects are important when the quantity $2\,(E/2mc^2)^2/(B/B_{cr})$ is small[5] (ie. for low temperatures and high field strengths), decreasing the rate below the value given by the asymptotic expression [Eqn (1b)]. The two-photon pair production rate has not been calculated in a magnetic field, so we have used the free-space rate, where the electron and positron states are assumed to be plane waves. The effect of the magnetic field might be estimated by examining the behavior of the inverse process, two-photon annihilation, which has been calculated in a strong magnetic field.[6] There is no significant deviation from the free-space rate until the field approaches 10^{13} G, and at this point, the one-photon annihilation rate begins to dominate. Therefore, from the preceeding argument, our calculation of the ratio of the two rates is probably most accurate below $B \sim 10^{13}$ G and at higher temperatures.

Photon distributions other than Maxwellian may be more realistic, since gamma-ray burst source emitting regions are not likely to be in equilibrium. The calculation presented here is meant only to give an idea of the relative behavior of the one- and two-photon processes. The actual rate of pair production in the source region would be an equilibrium solution including other processes affecting the distribution of photons and pairs, such as annihilation, synchrotron radiation and absorption, and Compton scattering. Comparisons such as this, however, may aid in the construction of the more self-consistent models by indicating which processes are important.

REFERENCES

1. E. P. Mazets, S. V. Golenetskii, R. L. Aptekar', Yu. A. Guryan, V. N. Ilinskii, Astrophys. Sp. Sci., 80, 119 (1981).
2. T. Erber, Rev. Mod. Phys., 38, 626 (1966).
3. T. A. Weaver, Phys. Rev. A, 13, 1563 (1976).
4. V. B. Berestetskii, E. M. Lifshitz, L. P. Pitaevskii, Relativistic Quantum Theory, (Pergamon, New York, 1971), p. 307.
5. J. K. Daugherty and A. K. Harding, Astrophys. J., in press (1983).
6. J. K. Daugherty and R. W. Bussard, Astrophys. J., 238, 296 (1980).

N83
2793

UNCLAS

N83 27931

ORIGINAL PAGE IS
OF POOR QUALITY

PAIR PRODUCTION AND ANNIHILATION IN STRONG MAGNETIC FIELDS

J. K. Daugherty
University of North Carolina-Asheville, Asheville, NC 28804

A. K. Harding
NASA/Goddard Space Flight Center, Greenbelt, MD 20771

ABSTRACT

Electromagnetic phenomena occurring in the presence of strong magnetic fields are currently of great interest in high-energy astrophysics. In particular, the process of pair production by single photons in the presence of fields of order 10^{12} Gauss is of importance in cascade models of pulsar gamma ray emission, and may also become significant in theories of other radiation phenomena whose sources may be neutron stars (e.g., gamma ray bursts). In addition to pair production, the inverse process of pair annihilation is greatly affected by the presence of superstrong magnetic fields. The most significant departures from annihilation processes in free space are a reduction in the total rate for annihilation into two photons, a broadening of the familiar 511-keV line for annihilation at rest, and the possibility for annihilation into a single photon (which dominates the two-photon annihilation for $B > 10^{13}$ Gauss). The physics of these pair conversion processes, which is reviewed briefly, can become quite complex in the teragauss regime, and can involve calculations which are technically difficult to incorporate into models of emission mechanisms in neutron star magnetospheres. However, recent theoretical work, especially in the case of pair annihilation, also suggests potential techniques for more direct measurements of field strengths near the stellar surface.

INTRODUCTION

The observational discovery of pulsars in the late sixties was rapidly followed by their identification with rotating magnetic neutron stars. Early models of these objects, in which the magnetic fields were postulated as the means by which the stellar rotational energy could be converted to electromagnetic radiation, in fact led to enormous estimates of the surface field strengths, on the order of 10^{12} Gauss or even more. Macroscopic fields of such intensity are roughly six orders of magnitude greater than the strongest attainable laboratory fields (which are currently the megagauss fields generated by implosive flux-compression techniques[1]). In fact, the field strengths thought to exist in the interiors and magnetospheres of neutron stars may well be the highest values occurring in nature.

In light of the fact that teragauss magnetic fields are so exotic by terrestrial standards, it is not surprising that the theory of electromagnetic phenomena occurring in such an environment is far from complete. Although many of the fundamentals in this area

PRECEDING PAGE BLANK NOT FILMED

ORIGINAL PAGE IS
OF POOR QUALITY

were investigated well before the discovery of pulsars[1], even these early investigations have only gradually become well known to astrophysicists. Hence a considerable amount of effort has been spent, especially in the last decade, on efforts both to increase our understanding of quantum electrodynamics in strong fields, and to incorporate this knowledge into specific models of neutron star magnetospheres and their emission mechanisms.

In this discussion we will review some recent developments in these areas, especially those relating directly to electron-positron pair conversion processes. The treatment is brief and incomplete, but is intended to convey roughly the level of our current knowledge of these processes, and to indicate some of the difficulties which this sort of physics presents to those interested in building models of pulsar cascade showers and other neutron star emission mechanisms.

QUANTUM ELECTRODYNAMICS IN STRONG MAGNETIC FIELDS

Although on a scale of the dimensions of a neutron star the magnetic field is certainly nonuniform, the length scale of interest in quantum electrodynamics is so much smaller (on the order of the Compton wavelength) that in calculations of electron-photon interactions the field may be considered perfectly uniform and infinite in extent. It may be noted that this is already a good approximation for typical accelerator magnets, and should in fact be much better for neutron star dimensions, whether these fields might be simply dipolar or of some more complex multipolar form. Moreover, the field is believed to be so intense that its treatment as a classical or prescribed "external" field (which is not itself influenced by the particle interactions) is also an excellent approximation. Hence the fundamental tool needed for calculating electromagnetic processes in neutron star magnetospheres is the quantum mechanical solution for electron/positron motion in a constant, uniform magnetic field. Fortunately this is one of the cases for which exact solutions of the relativistic Dirac equation are available[2]. We will not discuss the details of these wavefunctions here, but will concentrate on the energetics and kinematics associated with them.

The energy levels of a Dirac electron moving in a uniform magnetic field $\underline{B}$ may be written in the form

$$E_n = [c^2p^2 + m^2c^4(1 + 2nB/B_{cr})]^{1/2} \qquad (1)$$

where p denotes the component of momentum parallel to the field axis, $B_{cr} = m^2c^3/e\hbar = 4.414 \times 10^{13}$ Gauss, and n = 0, 1, 2, ... The form of this equation shows that the parallel momentum is not affected by the presence of the field, while the transverse motion is quantized. The critical field strength B_{cr} is seen to be a combination of fundamental constants whose value is such that a transition between adjacent orbitals produces an energy change comparable to the rest mass of the electron.

It is worth noting that the fully relativistic Dirac solutions

ORIGINAL PAGE IS
OF POOR QUALITY

to the equations of motion, which correspond to the energy level formula given above, should be preferred to the corresponding nonrelativistic Schrödinger wavefunctions in most applications to neutron star astrophysics. This is true in particular when either the parallel momentum p or the product $n\vartheta/B_{cr}$ becomes significant compared to the rest energy mc^2. For fields far below B_{cr}, the transverse energy becomes large only for enormous values of n (in which case the transitions to lower levels produce what is usually termed synchrotron radiation). However, at field strengths comparable to B_{cr}, even moderate values of n (normally associated with nonrelativistic "cyclotron" radiation) can produce effectively relativistic behavior.

Some obvious characteristics of the relativistic motion may be inferred from Figure 1, which shows the first few energy levels in a field of 5 teragauss. (Here the parallel momentum p has been set to zero.) As the figure indicates, each energy level above the ground state E_0 actually corresponds to two distinct spin states, which may be thought of as "up" or "down" along the field direction. It may be found from the relativistic Dirac wavefunctions that transitions involving spin flips are less probable than the corresponding "no-flip" transitions. However, the full set of spin states must be considered in determining the relative populations of excited states in neutron star magnetospheres. In addition, the decreasing spacings between levels for increasing quantum numbers n implies that multi-level populations will produce not only multiple harmonics of emission lines, but also line-splitting effects at each harmonic.

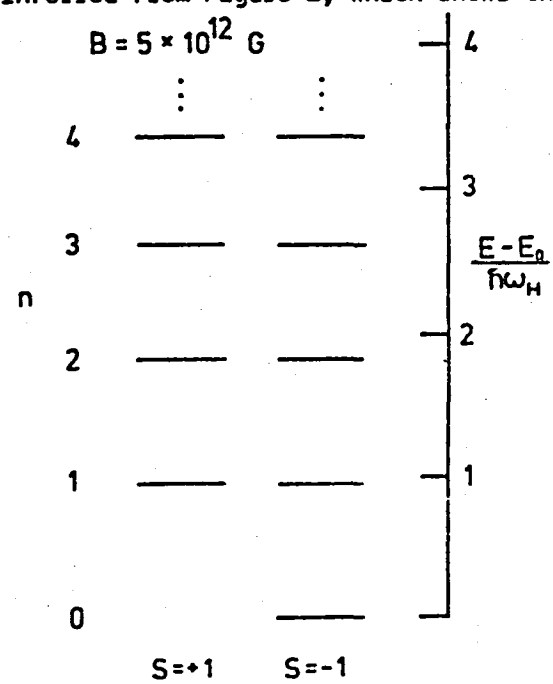

Fig. 1. Energy-level diagram for a Dirac electron in a uniform magnetic field of 5 teragauss. Here n is the orbital quantum number as given in eq. (1), and the parallel momentum p = 0. Scale at right is the energy spacing in units of cyclotron energy $\hbar\omega_H = e\hbar B/mc$.

In terms of perturbation theory calculations, pair production and annihilation effects in strong magnetic fields are described not only by the familiar second-order Feynman diagrams for these processes[3], but also by first-order diagrams involving only a single

ORIGINAL PAGE IS
OF POOR QUALITY

photon vertex. However, the meaning of "first-order" here must be clarified. In contrast to quantum electrodynamics in free space (where in fact all first-order processes are kinematically forbidden), the Dirac electron wavefunction itself fully describes the interaction with the constant, uniform magnetic field to all orders, while transitions induced by radiation-field photons are described by perturbation theory. The distinction is shown in Figure 2, which compares the second-order process of Bremsstrahlung in field-free space with the "first-order" process of magnetic Bremsstrahlung (synchrotron radiation) in a uniform magnetic field. (Note that there is a second contribution to case (a), in which the vertices are interchanged.) In (b) the electron interaction with the macroscopic B-field is depicted as an infinite number of zero-frequency photons, as opposed to the single "photon" associated with the microscopic Coulomb field of a nucleus in case (a).

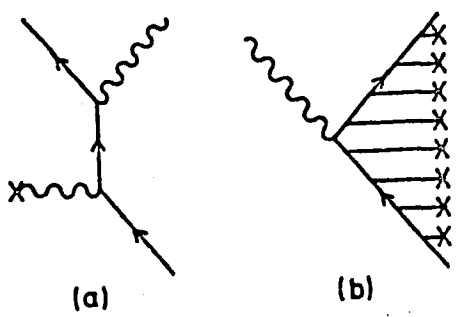

Fig. 2. Comparison of second-order diagram (a) for Bremsstrahlung in free space with "first-order" diagram (b) for magnetic Bremsstrahlung (synchrotron radiation) in external field.

Of the four possible ways to draw Feynman diagrams for first-order transitions, two represent just the familiar processes of synchrotron radiation and absorption. Obviously these effects are observable for fields far below the critical value B_{cr}, although it should be noted that the behavior of these effects in the strong-field regime is quite different from that associated with interstellar or accelerator fields[4-8]. However, the remaining two first-order processes, which are seen to be pair production and annihilation, are essentially quantum-mechanical effects and as such become significant (i.e., observable) only for fields approaching B_{cr}.

The kinematics of all the first-order transitions are determined by two equations, one for conservation of energy and one for conservation of parallel momentum:

$$\hbar\omega = E_j + E_k \tag{2a}$$

$$\hbar\omega \cos\theta/c = p + q \tag{2b}$$

where (E_j,p) and (E_k,q) are the total energy and parallel momenta of the positron and electron respectively, and Θ is the angle between the photon wave vector $\underline{k}$ and the field direction. There is no equation for the conservation of transverse momentum because the field itself participates in the transverse momentum transfer, and

ORIGINAL PAGE IS
OF POOR QUALITY

since the field lines are assumed to be infinitely "rigid" it is not possible to determine the transverse momentum exchange suffered by the particles. It is perhaps worth noting, however, that the rigidity of the field lines is also required to guarantee the conservation of total energy among the particles (equation 2a). In the case of neutron star magnetic fields, the assumption of infinitely rigid field lines is an extremely good approximation, since the field is both superstrong and and "anchored" (mechanically supported) by the mass of the star itself.

PAIR PRODUCTION

The process of magnetic pair production (the conversion of a single photon into an electron-positron pair in the presence of and external magnetic field) has been investigated by a number of authors[9-15], and the essential results have been known (although in some cases available only as unpublished doctoral theses) since the early fifties. The quantity of physical interest in dealing with this process is the attenuation coefficient (inverse of the mean free path) for a photon of specified energy ω and polarization vector $\underline{\varepsilon}$, propagating at some angle θ to the uniform magnetic field $\underline{B}$. (Henceforth natural units, in which $\hbar = c = 1$, will be assumed.) The actual calculation of the attenuation coefficient, based on the first-order Feynman diagram discussed above, may be performed in the Lorentz frame for which the photon motion is perpendicular to the field direction, with the understanding that the results (for unpolarized photons at least) may be generalized to arbitrary directions of propagation by making Lorentz transformations parallel to $\underline{B}$. We will follow this approach, but we must remember that the final step of transforming the results must eventually be performed in applications where $\underline{k}\cdot\underline{B} = 0$.

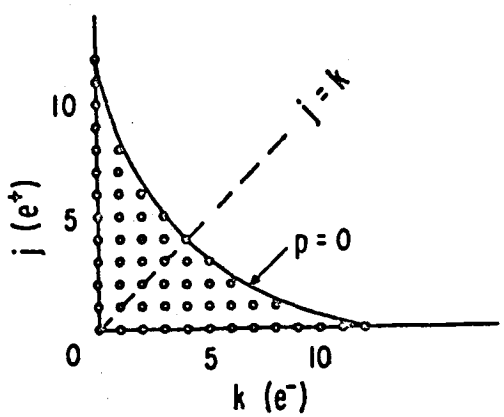

Fig. 3. Kinematically allowed states for the created e^+/e^- pair with quantum numbers (j,k).

Before we give the results of the dynamical calculations, it will be useful to consider the kinematic aspects of the pair production process. The final states of this process (namely the pair) may be labeled by two quantum numbers (j,k) describing the energy levels of the electron and positron respectively. As discussed in the preceding section, the kinematical requirements may be expressed as equations (2a,b). Now for a given photon energy and field strength B, these equations may be solved for the parallel momentum p:

ORIGINAL PAGE IS
OF POOR QUALITY

$$p = p(j,k) = \pm m\left[\omega'^2 - 1 - (j+k)B' + (j-k)^2 \frac{B'^2}{4\omega'^2}\right]^{1/2} \quad (3)$$

where $\omega' = \omega/2m$ and $B' = B/B_{cr}$. The energy-momentum restrictions are equivalent to the requirement that p^2 be a nonnegative number; for given ω and B, any pair states (j,k) which meet this requirement will be allowed. As shown in Figure 3, the region of allowed states in the (j,k) plane is thus enclosed within the line corresponding to the equation $p(j,k;\omega,B) = 0$. The sum of the individual transition rates for these final states will yield the attenuation coefficient for the pair conversion process. In addition, the relative probabilities for the various transitions over the (j,k) plane determine the energy distribution of the emergent pair, which is also of importance in applications (e.g., pulsar cascade models).

The explicit calculation of the attenuation coefficients in terms of the Dirac wavefunctions has been fully discussed in the references mentioned above and will not be repeated here. The results for the cases of photons whose electric vectors are polarized parallel and perpendicular to the field direction respectively are given by the expressions

$$R_{\parallel}(\omega',B') = \frac{\alpha_o}{2\xi}\sum_j\sum_k \frac{1}{|p_{jk}|}\{(E_jE_k + m^2 - p^2)(|M(j,k)|^2 + |M(j-1,k-1)|^2)$$

$$+ 2\sqrt{jk}\, B'm^2 [M^\dagger(j,k)\, M(j-1,k-1) + M^\dagger(j-1,k-1)\, M(j,k)]\} \quad (4a)$$

$$R_{\perp}(\omega',B') = \frac{\alpha_o}{2\xi}\sum_j\sum_k \frac{1}{|p_{jk}|}\{(E_jE_k + m^2 + p^2)(|M(j-1,k)|^2 + |M(j,k-1)|^2)$$

$$-2\sqrt{jk}\, B'm^2 [M^\dagger(j-1,k)M(j,k-1) + M^\dagger(j,k-1)M(j-1,k)]\} \quad (4b)$$

where $\xi = \frac{2\omega'^2}{B'}$, $M(j,k) = (-i)^{G-S}\sqrt{\frac{S!}{G!}}\, e^{-\xi/2}\, \xi^{\frac{G-S}{2}} L_S^{G-S}(\xi)$,

and $G = \max(j,k)$, $S = \min(j,k)$..

ORIGINAL PAGE IS
OF POOR QUALITY

At first glance these equations are not very illuminating, but from them we can immediately infer one important aspect of the behavior of the attenuation coefficients as functions of photon energy and field strength. The appearance of the momentum term p in the denominator of each summand implies that if any p vanishes, the entire expression becomes singular. Now from equation (3) it may be seen that for each integer pair (j,k), only certain combinations of and B can make p vanish. This in turn implies that for fixed B the attenuation coefficients $R(\omega,B)$ are singular at a discrete sequence of energies ω_{jk}, with each singularity resulting from particular (j,k) values for which p = 0. In terms of Figure 3, the attenuation coefficients are singular whenever ω and B are such that the line $p(j,k;\omega,B) = 0$ intersects an integer pair (j,k). Hence a plot of $R(\omega,B)$ vs. ω shows the sort of sawtooth behavior which is depicted in Figure 4. The energies at which the singularities occur are readily found from equation (3), and by plotting these energies it is found that the average spacing between peaks rapidly becomes smaller as the field strength is decreased, and that for fixed B the peaks in successive fixed-length energy intervals $d\omega$ become more numerous.

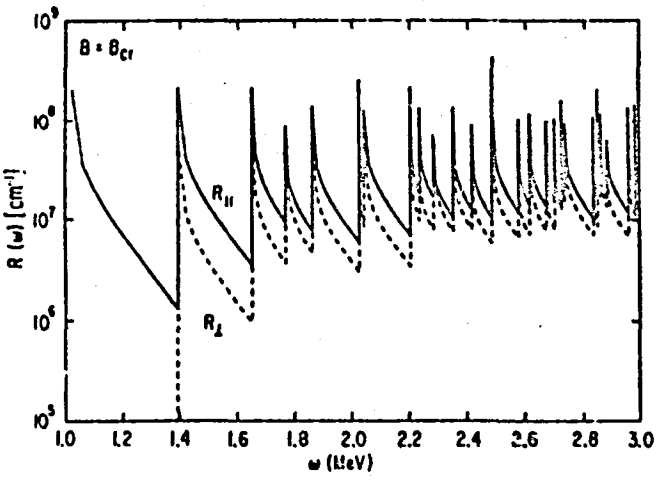

Fig. 4. Exact attenuation coefficients for photons propagating at right angles to the field direction and with polarizations parallel and perpendicular to the field, plotted vs. energy for fixed B (here chosen to be B_{cr}).

This complex behavior was noted even by the earliest authors who investigated this process[9,10], but for the maximum field strengths then considered to be of conceivable practical interest, the density of singularities in measurable energy intervals would be so great that only smoothed-out, average values taken over each interval were considered to be of physical interest. Hence asymptotic expressions for the attenuation coefficients, valid in the limiting regimes $\omega \gg 2m$ and $B \ll B_{cr}$, were derived from expressions (4). The crucial steps involved in this derivation are the replacement of the (j,k) summations by integrations over suitably chosen continuous variables, and the determination of appropriate asymptotic forms for the generalized Laguerre polynomials[9,10]. (For a recent discussion of this derivation, see reference[13].) The final results are expressible in the relatively

ORIGINAL PAGE IS
OF POOR QUALITY

simple form

$$\bar{R} \sim 0.23 \frac{\alpha_o}{\lambda\!\!\!^{-}_c} B' \exp\left(-\frac{4}{3\chi}\right), \qquad , \chi = \omega' B' << 1 \tag{5}$$

A comparison of the asymptotic results with the exact forms (4) for two sample field strengths in shown in Figure 5.

In most astrophysical applications to date, especially in models of cascade showers in pulsar magnetospheres[14,15], the last form of the attenuation coefficient has been used. Since the typical photon energies produced by curvature or synchrotron radiation in a cascade sequence are well above the MeV range, and the ambient field strengths are usually assumed to be no more than a few teragauss, the complex behavior for near-threshold energies and fields $B < B_{cr}$ has essentially been ignored. Moreover, the energy distribution of the pair has usually been assumed to be given simply by $E_{\pm} = \omega/2$. (It should also be noted that only unpolarized attenuation coefficients are used in these models.)

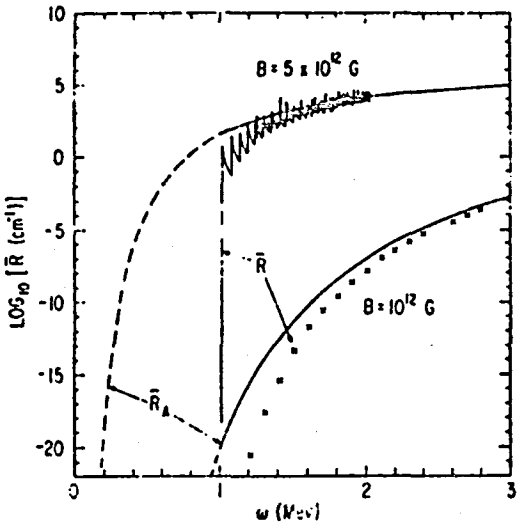

Fig. 5. Comparisons of exact (unpolarized) photon attenuation coefficients vs. asymptotic forms for 1- and 5-teragauss fields.

However, it turns out that this asymptotic form is often not a good approximation at all, since (as mentioned above) it is really necessary to Lorentz-transform the attenuation coefficients before they may be applied in frames for which $\underline{k}\cdot\underline{B}$ does not vanish. Now it turns out that the transformation law of the attenuation coefficients may be expressed as

$$\bar{R}\,(\omega, \underline{B}) = \sin\theta\, \bar{R}_o(\omega \sin\theta, \underline{B}) \tag{6}$$

This law expresses the fact that energetic photons, propagating at an angle $\theta \cong 1/\omega$ to the field direction, may be Lorentz-transformed down to energies near (or even below) threshold in the "transverse" frame for which $\underline{k}\cdot\underline{B} = 0$. But it is just such angles of propagation which are typical for the curvature-radiation photons which should inititate the pulsar cascade process. Hence a proper treatment of pair production by such photons must take into account the near-threshold effects, and the resulting modifications to the estimated multiplicities (ratios of secondary pairs to the number of radiating primary electrons drawn from the stellar

ORIGINAL PAGE IS
OF POOR QUALITY

surface) may have a significant effect on the entire cascade development. Moreover, it turns out that the energy distributions of the pairs in the near-threshold or high-field regimes, as determined by the individual contributions to expressions (4), can broaden considerably and even show double-peaked behavior as shown in Figure 6. (The double peaks imply that one member of the pair tends to get most of the photon energy, while the other emerges much closer to its ground state.) Hence the usual assumption that $E_{\pm} = \omega/2$ is also likely to be a poor approximation. This is unfortunately only one example where more careful treatments of the underlying processes in neutron star magnetospheres may force significant revisions to current models of their emission mechanisms.

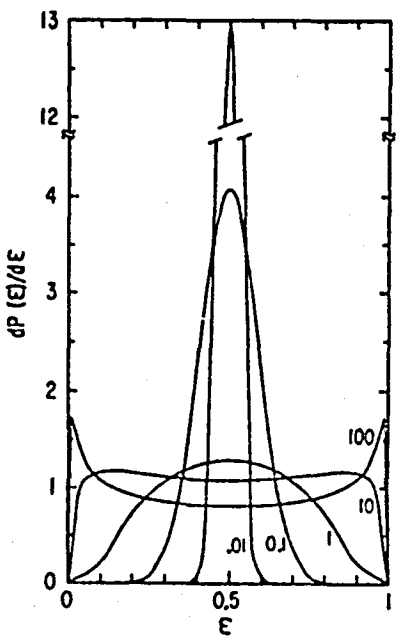

Fig. 6. Energy distributions for one member of the created pair, computed from an integration over the (j,k) probability distributions. The distributions shown are all normalized to unity, and are plotted vs. pair energy divided by photon energy.

PAIR ANNIHILATION

The inverse process of first-order pair production, namely pair annihilation into a single photon[16,17], is also of interest in neutron star astrophysics, but in this case the process becomes significant only for fields very close to B_{cr}. In weaker fields the first-order process is dominated by the analog of annihilation in free space, in which two or more photons make up the final state. The two-photon annihilation process, which will be discussed later below, is itself strongly modified by ambient fields of a few teragauss or more.

The kinematics for one-photon annihilation are similar to equations (2) for pair production, where the roles of initial and final states are now reversed. These equations imply that for annihilation by pairs at rest, the emergent radiation must form a flat fan beam at right angles to the field direction. For thermally

ORIGINAL PAGE IS
OF POOR QUALITY

or otherwise broadened e^+/e^- parallel momentum distributions, the fan beam would fill out to a form such as that shown in Figure 7. Corresponding to the angular distribution, the spectral distribution of the photon, assuming emission at specific angles, have characteristic asymmetrical shapes as shown in Figure 8. Both the overall shift toward higher energies and the increased broadening are due essentially to the Doppler effect caused by annihilation of pairs with nonzero net parallel momentum.

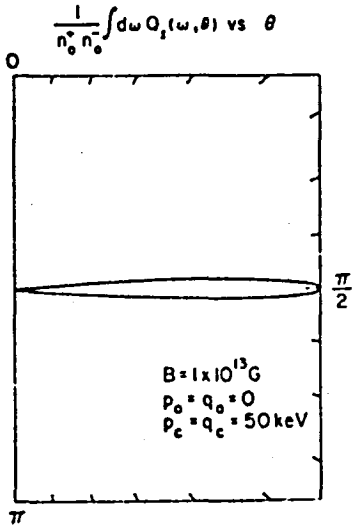

Fig. 7. Angular distribution of the one-photon annihilation radiation resulting from Gaussian electron-positron distributions with momentum widths of 50 keV, in a field of 10 teragauss (see reference 17).

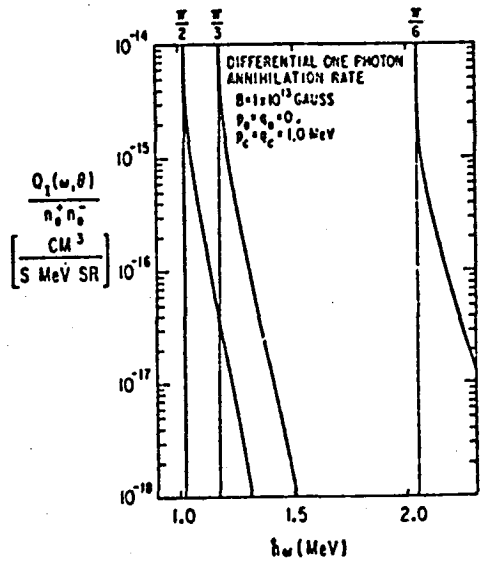

Fig. 8. Differential one-photon annihilation spectrum emitted from a ground-state gas of electrons and positrons with Gaussian parallel momentum distributions, here with widths of 1 MeV (reference 17). Separate spectra are shown for three angles of emission.

The kinematics for two-photon annihilation are more complex but are still characterized by a loss of transverse momentum conservation. As in the case of the first-order processes, the electron wavefunctions (and here the propagator as well) correspond to the Dirac constant-field wavefunctions. Several dynamical and kinematical aspects of two-photon annihilation turn out to be of special interest for neutron star astrophysics. The first is a reduction in the total annihilation rate as compared with the free-space value, accompanied by a flattening of the isotropic angular distribution of the emitted photons (tending toward a fan beam perpendicular to the field direction)[16]. In addition, the role of the field as a transverse momentum absorber leads to a sharply field-dependent broadening of the annihilation spectrum[17]. In

ORIGINAL PAGE IS
OF POOR QUALITY

particular, for annihilation at rest, the spectrum is no longer constrained by momentum conservation to the familiar 511-keV line, but is broadened to an extent which is quite sensitive both to field strength and angle of emission (see for example Figures 9,10). The line broadening is especially interesting in that it might become observable to detectors with high energy resolution for fields of only a few teragauss. Hence as a potential means for direct measurement of field strengths, the line-broadened two-photon annihilation spectrum might have wider usefulness. In this context it should be also be noted that the angular dependence of the broadening effects should, in beams emerging from local "hot spots" of rotating neutron stars, translate to a temporal dependence of the pulsed emission.

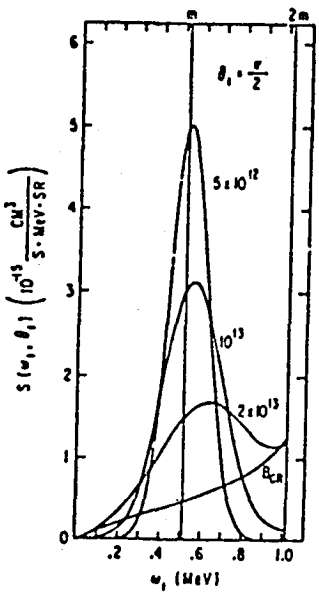

Fig. 9. Two-photon annihilation spectrum for pairs at rest, observed perpendicular to the field direction, for several field strengths above one teragauss. The sharply field-dependent line broadening is evident and is here due entirely to the loss of transverse momentum conservation in the intense field (i.e., no thermal broadening is included).

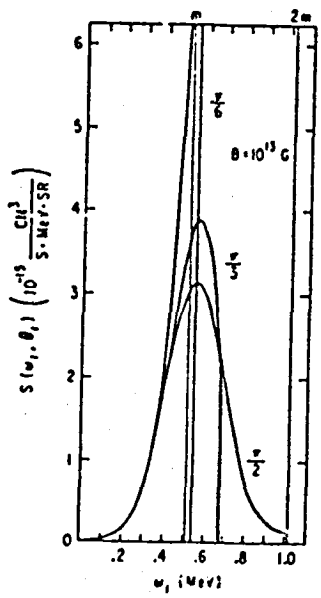

Fig. 10. Two-photon spectrum for annihilation at rest in a field of 10 teragauss, as viewed from several polar angles.

Finally, it should be noted that the range of field strengths over which the line broadening and overall rate decrease of the two-photon annihilation process becomes observable is really quite small, on the order of only one teragauss. The same statement holds

ORIGINAL PAGE IS
OF POOR QUALITY

for the "crossover" field strength (about 10 teragauss) at which the total one-photon annihilation rate begins to dominate the two-photon rate, as shown in Figure 11. Given this extreme sensitivity to the ambient field strength, it may eventually become possible for detectors with both high spectral and temporal resolution to provide accurate local values or even maps of the surface fields through the measurement of annihilation radiation.

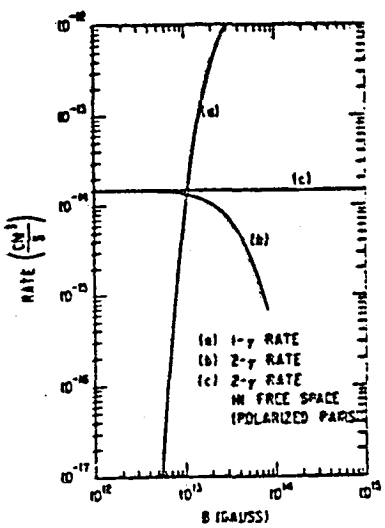

Fig. 11. Comparison of the total rates for annihilation into one and two photons at rest, as a function of field strength. The dashed line corresponds to the limit for two-photon annihilation at rest in free space, taking into account the fact that the electrons are in this case polarized as they would be in the ground state if the field is present.

CONCLUSION

The detailed physics of processes in teragauss magnetic fields, including the simple first- and second-order processes of the type discussed above, is still far from complete. The calculations of even the first-order processes involve a great deal of technical difficulties which are especially troublesome in the context of neutron star astrophysics, where often time-consuming calculations are already required to estimate emission spectra from the models. Indeed, it appears in many cases impractical to incorporate "exact" expressions such as equation (4) into models of pulsar cascades or gamma-ray burst sources, at least with computing resources that are less than what currently fall into the category of supercomputers. On the other hand, the analytical difficulties and pitfalls associated with attempts to improve or extend the asymptotic results for these processes are equally formidable, and the reliability of the results is open to question.

These same problems are only aggravated if we begin to consider various other fundamental processes, most of them intrinsically more complex than the simple pair conversion effects discussed here, which may also play significant roles in neutron star astrophysics. Among these may be mentioned such effects as the field-induced index of refraction[18,19], photon splitting[20], trident production[1], and such complications to the pair annihilation process as

ORIGINAL PAGE IS
OF POOR QUALITY

"magnetic" positronium formation and annihilation of positrons with the atomic electrons in the surface layers of the neutron star. At present, it is safe to say that the theoretical problems in this area will only slowly be put to rest.

At the same time, it is encouraging to note that even fairly elementary models of such processes as pulsar cascade showers[21] have already yielded reasonable agreement with the currently available observational data, in spite of the fact that the fundamental conversion processes have been treated in rather crude ways to date. Hence it may be that refinements to the theoretical treatments of these processes will only improve this agreement and not produce drastic or qualitative changes in the existing models. At present, however, it appears necessary not only to make the usual plea for more observational data, but also to emphasize the need for further theoretical investigations of the elementary processes of high-field physics and their careful treatment in models of pulsars, pulsating X-ray sources, and gamma-ray bursters.

REFERENCES

1. T. Erber, Rev. Mod. Phys. 38, 626 (1966).
2. See for example M. H. Johnson and B. A. Lippmann, Phys. Rev. 76, 828 (1949).
3. J. D. Bjorken and S. D. Drell, Relativistic Quantum Mechanics, (McGraw-Hill, N. Y.).
4. A. A. Sokolov and I. M. Ternov, Synchrotron Radiation, (Berlin: Akademie-Verlag), 1968.
5. H. G. Latal and T. Erber, Acta Phys. Austriaca
6. D. White, Phys. Rev. D 9, 868 (1974).
7. D. White, Phys. Rev. D 13, 1791 (1976).
8. J. K. Daugherty and J. Ventura, Phys. Rev. D 18, 1053 (1978).
9. J. S. Toll, Ph.D. thesis, Princeton University (1952).
10. N. P. Klepikov, Zh. Eksp. Teor. Fiz. 26, 19 (1954).
11. M. E. Rassbach, Ph.D. thesis, California Institute of Technology (1971).
12. Wu-yang Tsai and T. Erber, Phys. Rev. D 10, 492 (1974).
13. J. K. Daugherty and A. K. Harding, Astrophys. J., in press.
14. P. A. Sturrock, Astrophys. J. 164, 529 (1971).
15. M. A. Ruderman and P. G. Sutherland, Astrophys. J. 196, 51 (1975).
16. G. Wunner, Phys. Rev. Lett. 42, 79 (1979).
17. J. K. Daugherty and R. W. Bussard, Astrophys. J. 238, 296 (1980).
18. Wu-yang Tsai and T. Erber, Acta Phys. Austriaca 45, 245 (1976).
19. A. E. Shabad, Ann. Phys. (N. Y.) 90, 166 (1975).
20. S. L. Adler, Ann. Phys. (N. Y.) 67, 599 (1971).
21. J. K. Daugherty and A. K. Harding, Astrophys. J. 252, 337 (1982).

N83
27962

UNCLAS

N83 27932

D4

ORIGINAL PAGE IS
OF POOR QUALITY

LOW-TEMPERATURE POSITRON ANNIHILATION

Richard J. Drachman
Laboratory for Astronomy and Solar Physics
NASA/Goddard Space Flight Center, Greenbelt, MD 20771

ABSTRACT

For a satisfactory understanding of astrophysical annihilation radiation, expecially that observed from the galactic center direction, the interaction of positrons with the ambient medium must be carefully investigated. Although hot, ionized regions may be important sources of annihilation radiation, in this report I will examine mainly the simpler processes occurring in low-temperature neutral hydrogen gas. The goal is to set limits on conditions in the annihilation region by using the predictions of atomic theory compared with the observed γ-ray line width, continuum strength and time dependence.

INTRODUCTION

Suppose that positrons of energy high compared to the ionization energy of atomic hydrogen (13.6 eV) enter a region containing cold, non-ionized atomic hydrogen and nothing else. Assume further that no magnetic field or radiation is present in the region and that the hydrogen density is much less than 10^{12} cm^{-3}. We are thus considering a very simple, idealized model for the galactic center annihilation source and will try to predict the properties of the annihilation radiation emerging from this source. In spite of the simplicity of the model, it will be seen that a good deal of interesting physics is involved in its analysis. At the present time, there are no experimental data on the collision of positrons with atomic hydrogen, as there are for molecular hydrogen[1] and atomic helium.[2] On the other hand, the theoretical situation, although still imperfect, is relatively good, as I will show.

The observations[3-5] of the galactic center annihilation radiation are easily summarized:

1. A narrow line is seen; the best measurement[5] of its width (FWHM) gives 3.13 ± 0.57 keV. With a detector resolution of 2.72 keV, the source line width is 1.6(+0.9,-1.6) keV, consistent with zero.
2. The energy of the line is very accurately that expected for $e^+ - e^-$ annihilation at rest, 510.90 ± 0.25 keV compared with 511.00 keV in the laboratory.
3. There is some evidence[4] for the existence of a continuum component on the low-energy side of the line in addition to a power-law background.
4. The intensity of the line radiation is definitely time-variable,[5] with a time constant less than about 1/2 year.

In the next section the physical processes leading to annihilation of positrons will be described, and the resulting line

PRECEDING PAGE BLANK NOT FILMED

ORIGINAL PAGE IS
OF POOR QUALITY

width will be shown to be too large to agree with observations. The standard modification, allowing the annihilation region to be partly ionized will also be discussed. In the final section a possible loophole will be described, perhaps allowing retention of the original picture of a cold, non-ionized region and predicting some observational consequences. Much of the discussion below is based on the work of Bussard et al.[6] and Crannell et al.[7]

POSITRON ANNIHILATION

Five different reactions can occur in positron-hydrogen collisions at moderate energies (13.6 eV < E < 1 keV):

$e^+ + H \rightarrow e^+ + H$	(Elastic Scattering)	(1a)
$\rightarrow 2\gamma + H^+$	(Direct Annihilation)	(1b)
$\rightarrow e^+ + H^*$	(Excitation)	(1c)
$\rightarrow e^+ + e^- + H^+$	(Ionization)	(1d)
$\rightarrow Ps + H^+$	(Positronium Formation)	(1e)

Stecker[8] pointed out very early that in this energy range only the last process is effective in annihilating positrons, since Ps formation has an atomic-sized cross-section of order a_0^2 ($\sim 10^{-16}$cm^2) while process 1b is radiative, of order r_0^2 ($\sim 10^{-26}$cm^2). Essential to this argument is the low density of scatterers; once a Ps atom is formed it has no further collisions in the short time before it annihilates into 2 γ-rays (1.25×10^{-10} sec) or 3 γ-rays (1.4×10^{-7} sec). (The opposite occurs in most laboratory experiments where high densities are maintained; Ps formation in this energy range is merely an inelastic process, since the Ps atom is almost always collisionally ionized before it annihilates.)

With these considerations in mind, I can describe the life story of a positron very simply. It enters the cold atomic hydrogen region at some high energy and loses energy by processes (1c) and (1d). At about 100 eV process (1e) begins to become non-negligible, and for the rest of its lifetime every collision carries a certain increasing risk of Ps formation and immediate annihilation. It is the velocity distribution of the Ps atoms at the instant of their annihilation into 2 γ-rays that determines the width of the observed annihilation line. Before examining this question more quantitatively let us first note that positrons of energy E produce positronium atoms of energy $E - E_0$ (where $E_0 = 6.8$ eV, the threshold for process (1e) giving a rectangular distribution in the line-of-sight component of velocity v_z, ranging between $v_z = \pm\sqrt{(E-E_0)/m_e}$. Since the Doppler shift of one of the annihilation γ-rays is $\Delta = (v_z/c)m_ec^2$, one gets a rectangular line profile of width

$$\Gamma = 2\Delta = 1.430\sqrt{E(\text{ev})-6.80}\ \text{keV}. \qquad (2)$$

For this monoenergetic positron distribution to satisfy the

ORIGINAL PAGE IS
OF POOR QUALITY

experimental constraint $\Gamma \leq 2.5$ keV Eq. (2) requires $E \leq 9.86$ eV; we will see shortly that this is an unreasonably low energy.

In Ref. 6, a detailed Monte Carlo simulation is carried out, in which an ensemble of positrons is followed downward in energy until annihilation takes place. The resulting γ-ray line histogram corresponds to a width of 6.5 keV, in clear disagreement with observation. Rather than repeating the details here, I will use a simple continuous slowing-down model to describe the thermalization of the positrons. First, however, it is necessary to review the status of positron-hydrogen scattering theory, beginning with the Ps-formation cross-section.

This cross-section is difficult to compute accurately, in part because of the unsymmetrical relationship between initial and final states in Eq. (1e); the center of mass coordinate of the Ps atom is not a natural one for the initial e^+ - H state. Nevertheless, a number of two-channel calculations have been carried out both for s-waves[9] and p-waves,[10] and they agree in predicting a great reduction below the Born cross-section[11] for Ps formation, but they do not extend up to energies of interest here. For that reason, a phenomenological extension to higher energies was carried out,[12] which used a modified Born approximation whose L=0 and L=1 partial cross-sections were reduced to agree with Refs. 9 and 10, and whose L > 1 terms were unchanged. The only real test of this approximation comes from a comparison with the total inelastic cross-section of Winick and Reinhardt,[13] obtained by a sophisticated analytic technique. Although no distinction is made between Ps formation, excitation and ionization, only the first of these is energetically allowed for energies between 6.8 eV and 10.2 eV. There is reasonably good agreement in this energy range between the results of Refs. 12 and 13, encouraging me to use the results of Ref. 12 in the rest of the analysis. (Note that Ps formation in excited states has been neglected here; an increase of less than 20 percent might be expected in the cross-section at higher energy.)

I do not know of any positron-hydrogen ionization calculations (except for the Born approximation which does not distinguish e^+ from e^-.) A very simple analytic form has been devised by Lotz[14] for the e^- - H ionization cross-section:

$$\frac{\sigma_I}{\pi a_0^2} = \frac{2.47 \ln E \, [1 - 0.6 \, e^{-0.56(E-1)}]}{E} , \qquad (3)$$

where E is the energy in Rydbergs. I will use Eq. (3) in the analysis, although there is no estimate of error in the e^+ case.

On the other hand there is a recent close-coupling calculation of the positron impact cross-section for excitation of the n=2 levels of hydrogen.[15] Up to at least E = 7 Ry ($\approx$ 100 eV) these are well fitted by a formula like that of Eq. 3:

$$\frac{\sigma_{exc}}{\pi a_0^2} = \frac{2.73 \, (\ln (4/3 \, E) \, (1-0.63 \, e^{-0.531E})}{E} . \qquad (4)$$

ORIGINAL PAGE IS
OF POOR QUALITY

The n=2 excitation should dominate the total excitation process, so I will use Eq. (4) in the further analysis.

In Fig. 1 the Ps-formation cross-section and the inelastic scattering cross-section ($\sigma_I + \sigma_{exc}$) are plotted as functions of energy. To give an idea of the uncertainty in these quantities,

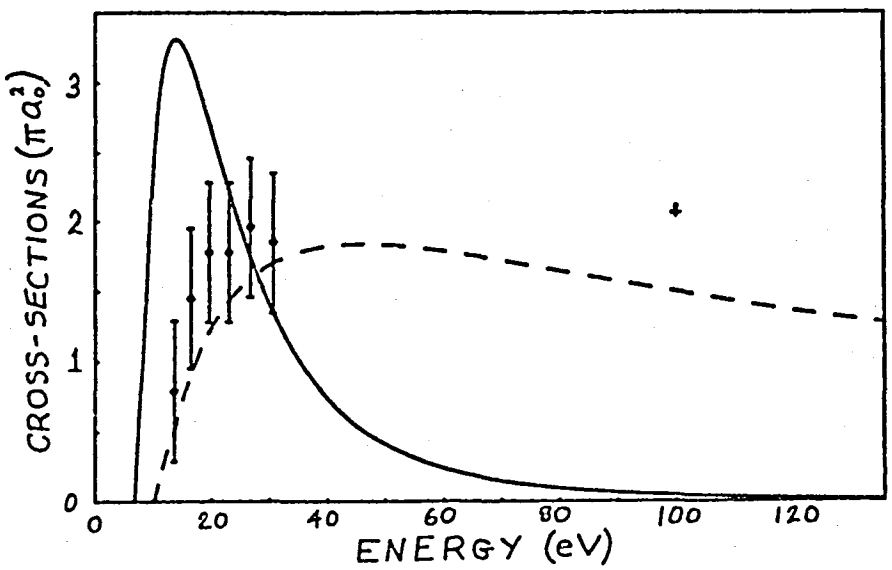

Fig. 1. Positron-hydrogen cross-sections as functions of energy. The solid line is for Ps formation (Ref. 12) and the dashed line is $\sigma_I + \sigma_{exc}$ (Eqs. 3 and 4). The dots and the cross are estimates of $\sigma_I + \sigma_{exc}$ obtained by combining the results of Ref. 12 with those of Ref. 13 and Ref. 16, respectively.

I have added a few additional points: the six low-energy points represent the difference bewteen total inelastic from Ref. 13 and Ps-formation from Ref. 12; the point at 100 eV is a similar result from an eikonal approximation.[16] These are both higher than the cross-section used here, but not, I think, in too serious disagreement; for atomic research more accuracy is desirable, but for astrophysics the present results are quite satisfactory.

Before carrying out a more detailed calculation of positron slowing down and γ-ray line shape I can draw some semi-quantitative conclusions from Figure 1 itself. Notice that the two competing processes, inelastic scattering and Ps formation, are equally probable at a positron energy of 28 eV. Of the positrons surviving to reach this energy one-half will form Ps at their next collision, and from Eq. (2) they will give a line width of 6.58 keV. It is thus unlikely that the observed width of $\Gamma \leq 2.5$ keV can be achieved.

To account correctly for the large energy losses occurring at each inelastic collision a Monte Carlo simulation is needed.[6] But an approximate, qualitatively correct treatment involving a

ORIGINAL PAGE IS
OF POOR QUALITY

continuous slowing-down approximation is easy to formulate and yields results much like the more exact ones. Assume that all positrons enter with the same high initial energy E_1 and lose energy according to the equation

$$\frac{dE}{dt} = -[\sigma_{exc}(E)\,\Delta_E + \sigma_I(E)\,\Delta_I]\,Nv(E) \tag{5}$$

where the cross-sections are from Eqs. 3 and 4, N is the number density of hydrogen and v is the positron velocity, $\sqrt{2E/m_e}$. The energy losses will be taken[6] as $\Delta_E = 10.2$ eV and $\Delta_I = 17$ eV. At the same time, the swarm of positrons is being depleted by Ps-formation following the equation

$$\frac{dn(E)}{dt} = -\sigma_{Ps}(E)\,n(E)\;\;v(E)\;\;N \tag{6}$$

These coupled equations can be integrated to give the time history of a positron swarm or the time dependence can be eliminated:

$$\frac{dn(E)}{dt} = \frac{dn(E)}{dE}\;\frac{dE}{dt}\;, \tag{7a}$$

$$\frac{dn(E)}{dE} = g(E)\;\;n(E), \tag{7b}$$

where $g(E) = \sigma_{Ps}(E)/[\sigma_{exc}(E)\,\Delta_E + \sigma_I(E)\,\Delta_I]$. Eq. (7b) has the trivial solution

$$n(E) = n(E_1)\,\exp\int_{E_1}^{E} dE'\;g(E')\;, \tag{8}$$

and I have plotted $n(E)/n(E_1)$ in Fig. 2, where $E_1 = 20\text{Ry} = 272\text{eV}$ is a high enough energy to be considered asymptotic, since $g(E_1)$ is very small. It is, of course, unrealistic to carry the solution below $E \approx \Delta_I$, since there the continuous slowing-down approximation is grossly incorrect.

The principal conclusion to be drawn from Fig. 2 is that the half-value energy, where only 1/2 of the original positrons still survive is at a high energy, $E_{1/2} = 39$ eV. This is a further indication that most of the Ps atoms formed are moving too fast to give the required narrow annihilation line. Furthermore, the exact line profile corresponding to this form of n(E) can be derived by integrating the rectangular line shapes of Eq. (2) normalized to an area proportional to dn(E). That is,

$$P(\Delta) \propto \int_{E_0+\Delta^2/m_ec^2}^{E_1} dE'\;g(E')n(E')\;/\sqrt{E'-E_0}\;. \tag{9}$$

ORIGINAL PAGE IS
OF POOR QUALITY

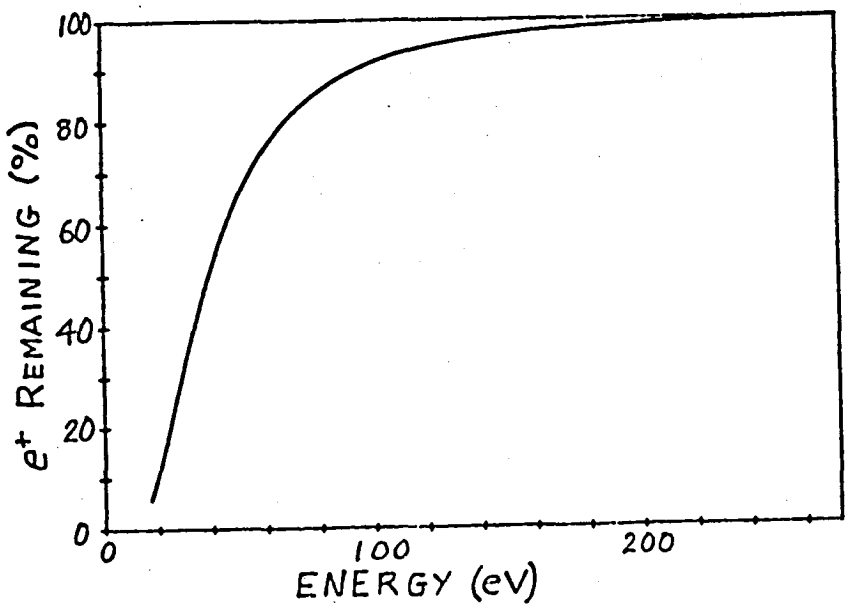

Fig. 2. Percent of positrons originally at 272 eV surviving to reach a given lower energy while slowing down in neutral atomic hydrogen.

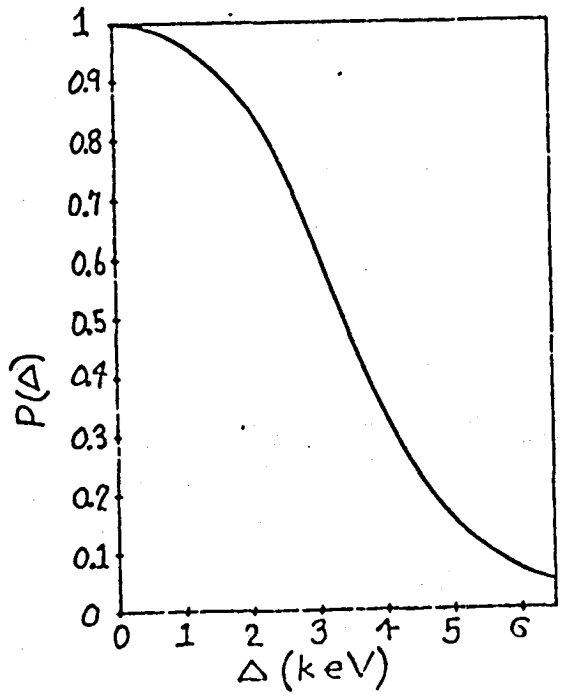

Fig. 3. Gamma-ray line intensity as a function of distance from the line center Δ. The line is symmetric about Δ = 0.

ORIGINAL PAGE IS
OF POOR QUALITY

In Fig. 3 I have plotted the annihilation line profile against Δ in keV. (The central parts of the line involving very low values of positron energy, where the present approximation is poor, have been extrapolated quadratically.) The width of the line calculated this way is 6.75 keV, in good agreement with the Monte Carlo results of Ref. 6, and once and for all inconsistent with the observations.

The solution to the dilemma is usually presented as follows[6]: If one allows some 5-10 percent ionization in the gas the slowing down of the positrons is so efficient that they do not form an appreciable amount of positronium before they take up a thermal velocity distribution. In Fig. 4 a diagram from Ref. 6 is reproduced. It shows the thermal-average rates for the four

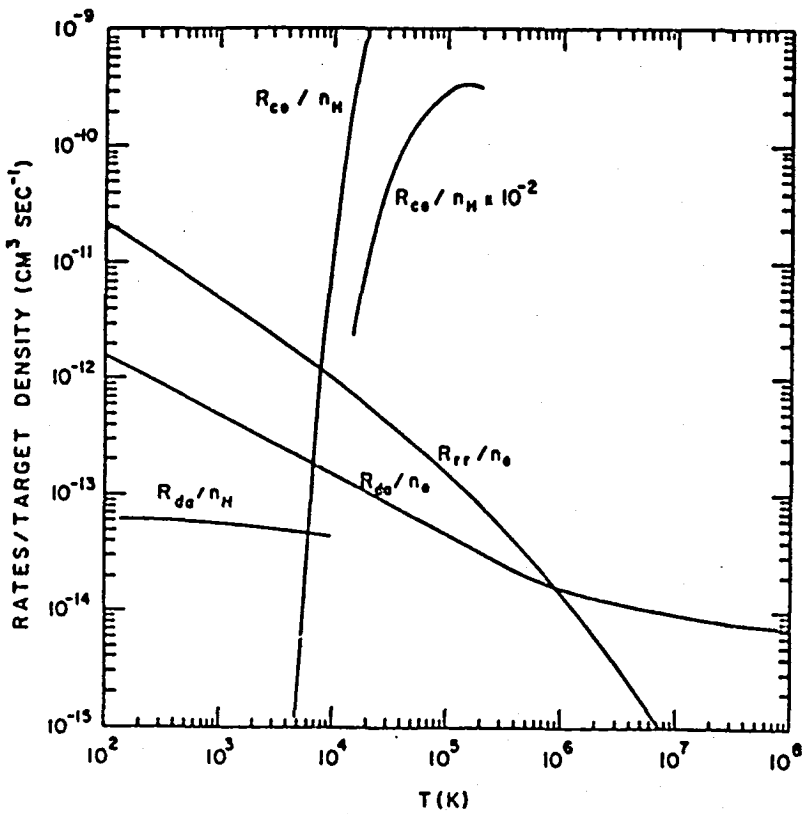

Fig. 4. Rates (per unit target density) at which thermal positrons form Ps by charge exchange with H (R_{ce}/n_H) or by radiative recombination with free electrons (R_{rr}/n_e), and annihilate directly with free electrons (R_{da}/n_e) or with bound electrons (R_{da}/n_H), as functions of temperature. (From Ref. 6)

ORIGINAL PAGE IS
OF POOR QUALITY

processes occurring in partially ionized hydrogen. At temperatures below about 5×10^3 K the dominant process is radiative recombination with an electron to form Ps followed by annihilation. The shape of the resulting line is

$$P(\Delta) = e^{-\Delta^2/kTm_ec^2} , \qquad (10)$$

its width is[7] $1.105\ (T_4)^{1/2}$ keV where T_4 is the temperature in 10^4K, and a satisfactory line width can be obtained. At higher temperatures charge exchange (Ps formation) with neutral hydrogen dominates; it rises very rapidly since only the tail of the thermal distribution above $E_0 = 6.8$ eV can contribute.

Once convinced that annihilation from a thermal swarm is occurring, we can, in principle determine the ionization fraction and the temperature if we know the line width and the Ps fraction. At present, of course, we have only an upper limit on the line width, while there is only rough and discordant data on the Ps fraction, which is obtained by a delicate process of curve fitting in the presence of a large γ-ray background. In Ref. 4 the most probable Ps fraction was given as 92 percent (but consistent with zero). At this Workshop, however, Riegler[17] suggested a value of about 20 ± 20 percent. Clearly no conclusion is yet possible. If the lower value proves to be correct, however, severe constraints will be placed on the scenario described above. In particular, it is not possible to keep the Ps fraction below about 60 percent while keeping the ionization fraction >5 percent. Several possible ways out of this dilemma would be to allow the annihilation to occur at high density[17] (to pick off the triplet Ps) or to flood the annihilation region with ultraviolet radiation (to ionize the triplet Ps before decay.) I will propose another possibility in the next section, by going back to the completely neutral case.

A TIME-DEPENDENT SOLUTION

In discussing Fig. 2, I did not mention the fact that about 5 percent of the original high-energy positrons avoid being annihilated as Ps during the slowing down process. This conclusion was originally drawn from the Monte Carlo calculation of Ref. 6, but a similar estimate can be obtained from Fig. 2. Note that the continuous slowing-down model should not be carried to an energy below 23.8 eV, since below that point a single ionization event will bring the positron below the Ps-formation threshold. But 19.0 percent of all the positrons reach 23.8 eV, and the probability that the next collision is an ionization event is $P_I(23.8) = \sigma_I(23.8) / [\sigma_I + \sigma_{exc} + \sigma_{Ps}] = 0.1335$. Similarly, the probability that the next collision is an excitation event is 0.2776, lowering the positron energy to 13.6 eV. At 13.6 eV, the excitation probability is 0.1303; in effect we are doing a very simple Monte Carlo calculation for the last few collisions before

ORIGINAL PAGE IS
OF POOR QUALITY

the Ps threshold is reached. The result is

$$n(E<5.8) = n(23.8)\ [P_I(23.8) + P_{exc}(23.8) \times P_{exc}(13.6)]$$

$$= 3.2 \text{ percent},$$

in qualitative agreement with Ref. 6. Three questions may be asked about this positron residue: how wide is the γ-ray line it produces, what is the resulting Ps fraction, and what is its time dependence

In this region ($E < 6.8$ eV) where energy loss is by elastic scattering only ($\Delta E/E = 2m_e/m_H$ per collision) and the annihilation rate is very low (due to collisions with H atoms), the continuous approximation is reliable. Using the almost exact e^+-H annihilation and momentum-transfer cross-sections[18] in the following equations

$$\frac{dE}{dt} = \frac{-2m_e\ \sigma_{MT}(E)\ Ev(E)N}{m_H} \tag{11}$$

$$\frac{dn(E)}{dt} = -\sigma_A(E)\ n(E)\ v(E)N \tag{12}$$

it is very easy to show that almost all the positrons cool rapidly and annihilate at very low evergy. (For example, 94 percent of all the positrons initially at 6.8 eV reach an energy of 0.05 eV, corresponding to about T = 600 K.) They will then annihilate with the bound electrons in the atomic hydrogen ground state; the quantum-mechanical momentum distribution is the cause of the annihilation line width, since the energy of the positrons is nearly zero.

If one has an accurate e^+-H zero-energy scattering wave function $\Psi(\vec{x}, \vec{r})$, where $\vec{x}$, $\vec{r}$ are the co-ordinates of incident e^+ and atomic e^- (in atomic units) respectively, the annihilation line profile is given by[19]

$$P(\Delta) \propto \int_{\frac{2\Delta}{\alpha m_e c^2}}^{\infty} dq\ q \left| \int d\vec{x}\ j_0(qx)\Psi(\vec{x}, \vec{x}) \right|^2. \tag{13}$$

Humberston[20] has carried out such a calculation, although with a different situation in mind, and from it an annihilation width of 1.3 keV can be derived. (Several references[6,21,22] have misquoted this as 2.6 keV.) This positron component gives a narrow annihilation line with a vanishingly small Ps component. (If some Ps is observed, a very small ionized fraction will account for it easily; at $T = 10^3$K, $n_e/n_H = 0.0025$ gives 20 percent Ps fraction.)

ORIGINAL PAGE IS
OF POOR QUALITY

In Ref. 6 we assumed that the broad line due to Ps formation and this narrow component were properly weighted and superposed, since we assumed a time-independent source. This combined annihilation line is not narrow enough to agree with the observations. The new suggestion I would like to make is based on the observed time dependence of the radiation.

Suppose a short burst of positrons is injected somehow into our cold atomic hydrogen region. We would observe two successive annihilation phases: The positrons would slow down in a relatively short time and, as described, would form Ps in flight giving a wide line at first. Soon, however, the only remaining positrons would be in the component below 6.8 eV, annihilating slowly with a narrow line width. From Eq. (12) it follows that if this second component is being observed $N > 10^6$ cm^{-3} for a mean life of 1/2 year. At this density the first phase should take less than 10 percent as long,[23] about one or two weeks. The conclusion is that randomly timed observations of the galactic center are much more likely to see narrow lines than wide ones, and this may be the explanation of the present observational situation.

It is important, then, to try to observe the galactic center source on a continuous basis, for the general purpose of charting its time dependence and specifically to look for the unique time dependence of the line width discussed above.

REFERENCES

1. K.R. Hoffman et al., Phys. Rev. A 25, 1393 (1982); M. Charlton et al., J. Phys. B 16, 323 (1983).
2. T.S. Stein et al., Phys. Rev. A 17, 1600 (1978); K.F. Canter et al., J. Phys. B 6, L 201 (1973); B. Jaduszliwer and D.A.L. Paul, Can. J. Phys. 52, 1047 (1974); G. Sinapius, W. Raith, and W.G. Wilson, J. Phys. B 13, 4079 (1980).
3. W.N. Johnson and R.C. Haymes, Astrophys. J. 184, 103 (1973); R.C. Haymes et al., Astrophys. J. 201, 593 (1975); F. Albernhe et al., Astron. Astrophys. 94, 214 (1981); M. Leventhal et al., Astrophys. J. 240, 338 (1980); M. Leventhal et al., Astrophys. J. 260, L1 (1982); W.S. Paciesas et al., Astrophys. J. 260, L7 (1982).
4. M. Leventhal, C.J. MacCallum, and P.D. Stang, Astrophys. J. 225, L 11 (1978).
5. G.R. Riegler et al., Astrophys. J. 248, L 13 (1981).
6. R.W. Bussard, R. Ramaty, and R.J. Drachman, Astrophys. J. 228, 928 (1979).
7. C.J. Crannell et al., Astrophys. J. 210, 582 (1976).
8. F.W. Stecker, Cosmic Gamma Rays (NASA, Washington, 1971). "Ps" is the chemical symbol for positronium, the hydrogen-like atom composed of one positron and one electron. Its two possible spin states annihilate into 2 γ-rays (singlet) or 3 γ-rays (triplet).

ORIGINAL PAGE IS
OF POOR QUALITY

9. J. Stein and R. Sternlicht, Phys. Rev. A 6, 2165 (1972); Y.F. Chan and P.A. Fraser, J. Phys. B 6, 2504 (1973); J.W. Humberston, Can. J. Phys. 60, 591 (1982).
10. Y.F. Chan and R.P. McEachran, J. Phys. B 9, 2869 (1976).
11. H.S. W. Massey and C.B.O. Mohr, Proc. Phys. Soc. (London) A 67, 695 (1954); I.M. Cheshire, Proc. Phys. Soc. 83, 227 (1964).
12. R.J. Drachman, K. Omidvar, and J.H. McGuire, Phys. Rev. A 14, 100 (1976).
13. J.R. Winick and W.P. Reinhardt, Phys. Rev. A 18, 925 (1978).
14. W. Lotz, Z. fur Physik 206, 205 (1967).
15. L.A. Morgan, J. Phys. B 15, L 25 (1982).
16. F.W. Byron, Jr., C.J. Joachain, and R.M. Potvliege, J. Phys. B 15, 3915 (1982).
17. G.R. Riegler, this volume.
18. A.K. Bhatia, R.J. Drachman and A. Temkin, Phys. Rev. A 16, 1719 (1977).
19. R.J. Drachman, in VII ICPEAC, Invited Talks and Progress Reports edited by T.R. Govers and F.J. de Heer (North-Holland, Amsterdam, 1972), p. 277.
20. J.W. Humberston and J.B.G. Wallace, J. Phys. B 5, 1138 (1972).
21. R.J. Drachman, Can. J. Phys. 60, 494 (1982).
22. R.J. Drachman, in Positron Annihilation edited by P.G. Coleman, S.C. Sharma, and L.M. Diana (North-Holland, Amsterdam, 1982), p. 37.
23. R.E. Lingenfelter and R. Ramaty, in The Galactic Center edited by G.R. Riegler and R.D. Blandford (Am. Inst. Phys., NY, 1982).

N83
27933

UNCLAS

ORIGINAL PAGE IS
OF POOR QUALITY

N83 27933

D5

UPPER LIMITS TO THE ANNIHILATION RADIATION LUMINOSITY OF CENTAURUS A

N. Gehrels*, T. L. Cline, W. S. Paciesas+**,
B. J. Teegarden, and J. Tueller**
NASA/Goddard Space Flight Center, Greenbelt, MD 20771

P. Durouchoux and J. M. Hameury
Centre d'Etudes Nucléaires de Saclay, France

ABSTRACT

A high-resolution observation of the active nucleus galaxy Centaurus A (NGC 5128) was made by the GSFC Low Energy Gamma-ray Spectrometer (LEGS) during a balloon flight on 1981 November 19. The measured spectrum between 70 and 500 keV is well represented by a power law of the form 1.05×10^{-4} (E/100 keV)$^{-1.59}$ ph cm^{-2} s^{-1} with no breaks or line features observed. The 98% confidence (2σ) flux upper limit for a narrow (< 3 keV) 511-keV positron annihilation line is 9.9×10^{-4} ph cm^{-2} s^{-1}. Using this upper limit, the ratio of the narrow-line annihilation radiation luminosity to the integral > 511 keV luminosity is estimated to be < 0.09 (2σ upper limit). This is compared with the measured value for our galactic center in the Fall of 1979 of 0.10-0.13, indicating a difference in the emission regions in the nuclei of the two galaxies.

INTRODUCTION

Centaurus A (NGC 5128) is a nearby galaxy (~ 5 Mpc) with an active nucleus that is an intense source of X-rays and gamma-rays. The nuclear source is variable on time scales from days to years and is spatially unresolved at X-ray energies; the upper limit to the size of the nuclear component of the X-ray emission is 0.3 arcsec[1] (8 pc). Einstein observations indicate that above ~ 2 keV the nuclear component dominates the X-ray emission from the galaxy[1].

There are three previously reported observations of Cen A by instruments capable of measuring a positron annihilation feature in the spectrum: the Rice University instrument in 1968[2] and 1974[3], and HEAO A-4 in 1978[4]. No lines were seen at 511 keV in any of the three observations, with 2σ flux upper limits for an unresolved line being 1.8×10^{-3}, 8×10^{-4}, and 6.5×10^{-4} ph cm^{-2} s^{-1}, respectively. These instruments employed scintillation detectors with energy resolutions at 511 keV in the 40-70 keV FWHM range. We report here the results of the first high-resolution gamma-ray observation of Cen A, made by an instrument employing Germanium detectors with a resolution of 2.2 keV FWHM at 511 keV.

* NAS/NRC Resident Research Associate
+ Present Address: Department of Physics, University of Alabama, Huntsville, AL 35899
** Also the University of Maryland

PRECEDING PAGE BLANK NOT FILMED

ORIGINAL PAGE IS
OF POOR QUALITY

OBSERVATIONS

The GSFC Low Energy Gamma-ray Spectrometer (LEGS) performs high-resolution spectroscopy between ~ 70 keV and 8 MeV using an array of three cooled high-purity Ge detectors surrounded by an active NaI scintillation shield. The detectors have an active volume of 230 cm^3 and a peak effective area of 35.5 cm^2 at 130 keV. The average in-flight energy resolution rises from 1.8 keV FWHM at 70 keV to 3.5 keV at 2.6 MeV. At 511 keV the effective area is 13.3 cm^2, and the resolution is 2.2 keV FWHM. The active NaI shield is ~ 12 cm thick and collimates the field-of-view of the detectors to ~ 16° FWHM. The instrument is balloon-borne and is mounted in a servo-controlled gondola that uses an altazimuth pointing system under microcomputer control; the pointing precision is ~ 0.5°. A detailed description of LEGS is given by Paciesas et al.[5].

The instrument was launched from Alice Springs, Australia on 1981 November 19 and observed Cen A for 3 hours at an average line-of-sight atmospheric depth of 3.5 g cm^{-2}. The observation was divided into 20-minute intervals during which the telescope was alternately pointed at the source and away from the source for background determination. The source flux was calculated by subtracting the average background level from each source interval, correcting for detector efficiency and atmospheric attenuation, and summing the resulting residual fluxes.

Figure 1 shows the observed spectrum of Cen A, calculated as described above. The best-fitting power law of the form $A(E/100\ \mathrm{keV})^{-\alpha}$ has $A = 1.05 \times 10^{-4}$ ph cm^{-2} s^{-1} keV^{-1} and $\alpha = 1.59$. The joint 90% confidence error limits ($\chi^2_{min} + 4.6$; reference 6) for A and α are shown in the inset. The data are consistent over the entire measured energy range with a power law of photon index − 1.59, showing no evidence for a spectral break. The observed values of A and α are both intermediate in the range of values measured previously for Cen A (reference 4, and references therein).

The data were searched for features in the spectrum with the result that no statistically significant narrow or broad lines were seen. The 2σ flux upper limit for a narrow (< 3 keV FWHM) 511-keV positron annihilation line is 9.9×10^{-4} ph cm^{-2} s^{-1}, calculated from the source flux in a 4-keV wide bin[7] centered on 511 keV. This limit is a factor of ~ 1.9 larger than the upper limits at nearby energies due to the intense instrumental background line at 511 keV[5].

DISCUSSION

The lack of a 511-keV line in the Cen A spectrum is of particular interest in light of the 511-keV emission that has been observed from the central region of our own galaxy (see, e.g., reference 8). In order to compare the nucleus of Cen A with the galactic center source, we calculate here the ratio of the 511-keV line luminosity (or upper limit to the luminosity) to the luminosity of photons with energies > 511 keV. This second quantity is not as accurately determined for either source as lower-energy integrals of

ORIGINAL PAGE IS
OF POOR QUALITY

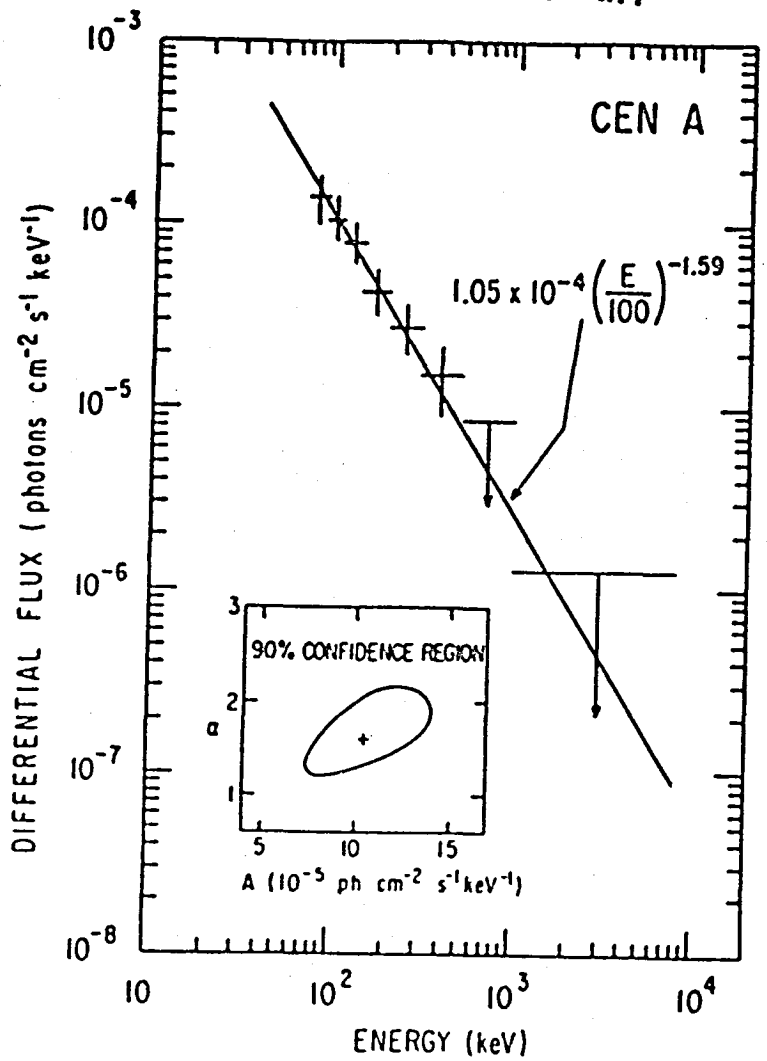

Figure 1. Cen A spectrum and best-fitting power law. The points between 70 and 500 keV are shown with 1σ statistical error bars, while the upper limits between 500 keV and 8 MeV are 2σ (98 percent confidence) upper limits. Inset--90 percent confidence contour for power-law parameters A and α defined in text.

ORIGINAL PAGE IS
OF POOR QUALITY

the spectra but is more relevant for the comparison; for instance, the positrons responsible for the galactic center 511-keV emission are likely produced by γ-γ interactions of photons with $\gtrsim m_e c^2$ energies[9]. Also, for the galactic center region there is considerable source confusion in the low-energy gamma-ray measurements made to date, whereas at energies greater than a few hundred keV the nuclear source dominates[10].

Since no flux measurements exist for Cen A between 1 MeV and 1 GeV, an extrapolation of our measured spectrum (Figure 1) was required to obtain the Cen A luminosity at energies > 511 keV. We performed the extrapolation using the spectral form for the differential flux

$$\frac{dF}{dE} = \frac{0.159}{E^{1.59}[1 + (E/2000\ \text{keV})^{1.3}]}\ \text{photons cm}^{-2}\ \text{s}^{-1}\ \text{keV}^{-1} \qquad (1)$$

in analogy to the observed spectrum for 3C 273[11,12]. The spectral form in equation (1) tends toward the measured spectrum below 1 MeV and is consistent with the SAS-2 flux upper limits[12] between 35 and 200 MeV. Based on equation (1), the Cen A luminosity at energies > 511 keV is 2.7×10^{43} ergs s^{-1}. The LEGS 2σ upper limit for narrow-line 511-keV emission of 9.9×10^{-4} ph cm^{-2} s^{-1} gives a line luminosity upper limit of 2.4×10^{42} ergs s^{-1}. The upper limit for the line-to-continuum ratio is, therefore, 0.090; a similar analysis using the HEAO A-4[4] line limit and spectrum gives a ratio upper limit of 0.073.

For the galactic center, we use the HEAO C-1 observations in the Fall of 1979. Depending on the assumption of the shape of the spectrum, the > 511 keV luminosity is in the range $1.4\text{-}1.7 \times 10^{38}$ ergs s^{-1}, based on data extending above 1 MeV (G. Riegler, private communication, 1983). The measured narrow-line 511-keV luminosity at that time was $(1.8 \pm 0.2) \times 10^{37}$ ergs s^{-1} [13], yielding a line-to-continuum ratio in the approximate range 0.10-0.13. Both the line and continuum fluxes from the galactic center are variable[13,14] with the line flux falling below detectable levels in recent measurements[15,16]. However, there is evidence for a correlation betwen the line and continuum flux levels[14,16] so that the line-to-continuum ratio of ~ 0.12 may apply to other times than the Fall 1979 measurement. Both the LEGS and HEAO A-4 2σ upper limits for the Cen A line-to-continuum ratio fall below the measured galactic center ratio. Their combined weight gives evidence that the emission regions in the nuclei of the two galaxies are different. This result is not surprising given the factor of ~ 10^5 difference in gamma-ray luminosity of the two sources. The higher temperature and activity level that one might expect in the nucleus of Cen A could produce a broadening of any 511-keV line emission. None of the observations to date have detected a broadened annihilation-radiation feature in the spectrum, but the sensitivity for line detection decreases as the line width increases above the instrumental resolution width.

ORIGINAL PAGE IS
OF POOR QUALITY

SUMMARY

Cen A was observed on 1981 November 19 with a high-resolution gamma-ray spectrometer. The photon spectrum between 70 and 500 keV was found to be well fit by a power law of the form 1.05×10^{-4} $(E/100\ \mathrm{keV})^{-1.59}$, with no evidence of a break. No lines or features were seen in the spectrum; the 2σ flux upper limit for a narrow (< 3 keV) 511-keV positron-annihilation line is 9.9×10^{-4} ph cm^{-2} s^{-1}. A comparison with the observed 511-keV line flux from the galactic center in the Fall of 1979 indicates that Cen A is less luminous than the galactic center in 511-keV narrow-line emission relative to the > 511 keV continuum emission.

REFERENCES

1. E. D. Feigelson, E. J. Schreier, J. P. Delvaille, R. Giacconi, J. E. Grindlay, and A. P. Lightman, Ap. J. 251, 31 (1981).
2. R. C. Haymes, D. V. Ellis, G. J. Fishman, S. W. Glenn, and J. D. Kurfess, Ap. J. 155, L31 (1969).
3. R. D. Hall, C. A. Meegan, G. D. Walraven, F. T. Djuth, and R. C. Haymes, Ap. J. 210, 631 (1976).
4. W. A. Baity, R. E. Rothschild, R. E. Lingenfelter, W. A. Stein, P. L. Nolan, D. E. Gruber, F. K. Knight, J. L. Matteson, L. E. Peterson, F. A. Primini, A. M. Levine, W. H. G. Lewin, R. F. Mushotzky, and A. F. Tennant, Ap. J. 244, 429 (1981).
5. W. Paciesas, et al., submitted to Nucl. Inst. Meth. (1983).
6. M. Lampton, B. Margon, and S. Bowyer, Ap. J. 208, 177 (1976).
7. A. S. Jacobson, R. J. Bishop, G. W. Culp, L. Jung, W. A. Mahoney, and J. B. Willett, Nucl. Inst. Meth. 127, 115 (1975).
8. M. Leventhal, C. J. MacCallum, and P. D. Stang, Ap. J. 225, L11 (1978).
9. R. E. Lingenfelter and R. Ramaty, in The Galactic Center, ed. G. R. Riegler and R. D. Blandford (New York: Am. Inst. Phys.), p. 148.
10. J. L. Matteson, in The Galactic Center, ed. G. R. Riegler and R. D. Blandford (New York: Am. Inst. Phys.), p. 109.
11. B. N. Swanenburg, K. Bennett, G. F. Bignami, P. Caraveo, W. Hermsen, G. Kanback, J. L. Masnou, H. A. Mayer-Hasselwander, J. A. Paul, B. Sacco, L. Scarsi, and R. D. Wills, Nature 275, 298 (1978).
12. G. F. Bignami, C. E. Fichtel, R. C. Hartman, and D. J. Thompson, Ap. J. 232, 649 (1979).
13. G. R. Riegler, J. C. Ling, W. A. Mahoney, W. A. Wheaton, J. B. Willett, A. S. Jacobson, and T. A. Prince, Ap. J. 248, L13 (1981).
14. G. R. Riegler, J. C. Ling, W. A. Mahoney, W. A. Wheaton, and A. S. Jacobson, 17th Int. Cosmic Ray Conf. 9, 85 (1981).
15. M. Leventhal, C. J. MacCallum, A. F. Huters, and P. D. Stang, Ap. J. 260, L1 (1982).
16. W. S. Paciesas, T. L. Cline, B. J. Teegarden, J. Tueller, P. Durouchoux, and J. M. Hameury, Ap. J. 260, L7 (1982).

N83
27934

UNCLAS

ORIGINAL PAGE IS
OF POOR QUALITY

N83 27934

PAIR PRODUCTION NEAR THRESHOLD IN PULSAR MAGNETIC FIELDS

A. K. Harding
NASA/Goddard Space Flight Center, Greenbelt, MD 20771
and
J. K. Daugherty
University of North Carolina, Asheville, NC 28804

ABSTRACT

In pulsar polar cap models, curvature radiation γ-rays produce e^+e^- pairs in the strong magnetic fields near the surface of the neutron star. While these γ-rays have energies $E_\gamma \gg mc^2$, they also propagate at very small angles to the field, such that the threshold condition, $E_\gamma > 2mc^2/\sin\theta$ is just barely satisfied when they pair produce. Threshold effects on the pair production attenuation coefficient, which are due to the discreteness of the e^+e^- Landau states, must therefore be considered when computing the mean free paths of curvature radiation photons in pulsar magnetic fields. These effects, which are not incorporated in the asymptotic expression for the attenuation coefficient, have some interesting consequences for pulsar models. Since pair production is suppressed near threshold, the photon mean free paths are longer than previously thought. In magnetic fields $\gtrsim 6\times10^{12}$ G, the pairs tend to be produced in the ground state Landau level and will not synchrotron radiate. Since synchrotron radiation is an essential ingredient in the electromagnetic cascades which produce low energy pairs above the acceleration region, pulsars with very high magnetic fields may not produce many pairs.

INTRODUCTION

The production of e^+e^- pairs plays a central role in most current pulsar models. Polar cap voltage drops which accelerate particles to ultrarelativistic energies are limited by pair production discharges,[1,2,3] which continue in the form of electromagnetic cascades above the acceleration region.[4] These pair-photon cascades can generate large numbers of e^+e^- pairs which are thought to be essential for the coherent radio emission process. The most important mechanism for producing pairs near the polar cap is pair production by single photons in the intense magnetic field of the neutron star. Recent theoretical study of this process has provided a description of the behavior of the photon attenuation coefficient near threshold and the energy distribution of the pairs.[5,6] In this paper, we discuss the implication of these results for pair production and electromagnetic cascades in pulsar magnetospheres.

PHOTON MEAN FREE PATHS

Magnetic pair production has been studied extensively, and almost exclusively, in the asymptotic limit of low fields, $B \ll B_{cr}$, and high photon energies $\hbar\omega \gg 2mc^2$, where $B_{cr} \equiv 4.414 \times 10^{13}$G is

PAGE BLANK NOT FILMED

ORIGINAL PAGE IS
OF POOR QUALITY

the critical field strength. If we define the units $\omega' \equiv \omega/2m$ and $B' \equiv B/B_{cr}$ ($\hbar = c = 1$), then this limit takes the form, $\xi \equiv 2\omega'^2/B' \to \infty$. The parameter ξ is related to the number of energetically allowed Landau states available to the e^+e^- pair. In this limit, the polarization-averaged photon attenuation coefficient in the "center of mass" frame, where the photon propagates perpendicular to B, is[7]

$$R_{CM}(\omega',B') \sim 0.23 \frac{\alpha}{\hbar} B' \exp\left(\frac{-4}{3\chi}\right) \text{ cm}^{-1}, \quad \chi \ll 1 \qquad (1)$$

where $\chi \equiv \omega'_{CM} B'$. In an arbitrary frame, where the photon propagates at an angle θ to B, its energy can be found by Lorentz transforming along B with velocity, $\beta = \cos\theta$, and the result is $\omega' = \omega'_{CM}/\sin\theta$. Similarly, the attenuation coefficient becomes $R = \sin\theta\, R_{CM}$.

To produce a pair, the photon center of mass energy must exceed threshold energy and the attenuation coefficent must be non-negligible. These two conditions are independent and can be expressed in the following simple forms:

(A) $\omega_{CM} = \omega \sin\theta \geq 2m$

(B) $\chi \gtrsim 0.1$

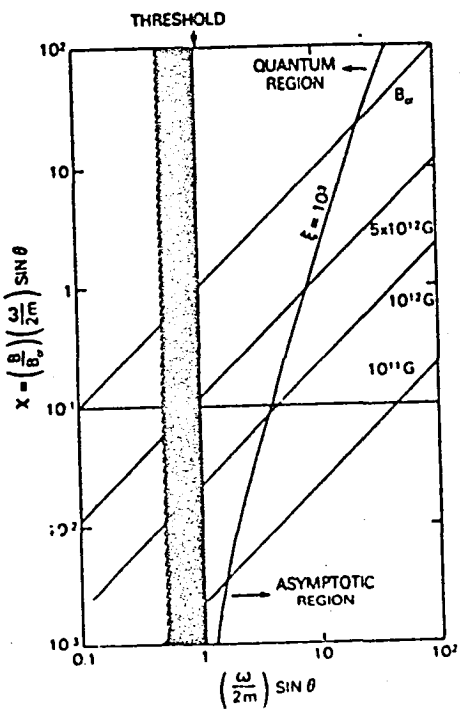

where the latter comes from the exponential dependence of $R(\omega', B')$. Figure 1 illustrates where these conditions are satisfied for different field strengths.

In pulsar magnetospheres, high energy particles produce curvature radiation photons at very small angles to the field such that $\omega\sin\theta < 2m$ even though $\omega \gg 2m$. In order to pair produce, then, these photons must propagate in a straight path until they acquire an angle to the curved field lines which satisfies (A). In figure 1, this is equivalent to moving upward along the diagonal lines of constant field strength. If (B) is satisfied before (A), as it is for $B \gtrsim 0.1\, B_{cr} = 4.4 \times 10^{12}$ G, then the photon will pair produce very near threshold, where Eqn (1) is no longer accurate. It has been

Fig. 1. Pair production parameter χ vs. "center of mass" photon energy for different field strengths(diagonal lines).

ORIGINAL PAGE IS
OF POOR QUALITY

found (Ref. 5) that the quantum effects of the discrete pair states suppress the pair production attenuation coefficient below the asymptotic limit, such that a more accurate expression is:

$$R_{CM}(\omega', B') \sim 0.23 \frac{\alpha}{\lambda\!\!\!^{-}} B' \exp\left[\frac{-4 f(\omega'_{CM}, B')}{3\chi}\right] cm^{-1}, \quad \omega'_{CM} \geq 1$$

$$f(\omega'_{CM}, B') \approx 1 + .42\, \omega'^{-2.7}_{CM}\, B'^{-.0038} \tag{2}$$

The function $f(\omega', B')$ approximates the behavior of the exact attenuation coefficient near threshold, after averaging over the sawtooth pattern of cyclotron resonance spikes (cf. Ref. 6).

Since $\sin\theta$ increases with the photon path length, s, approximately as s/ρ, where ρ is the radius of curvature of the magnetic field, the mean free paths of the photons, from either condition (A) or (B) and Eqn (2) will be

$$\frac{\lambda}{\rho} \approx \frac{0.1\, f(\omega'_{CM}, B')}{\omega' B'}, \qquad B' \lesssim 0.1 \tag{3a}$$

$$\frac{\lambda}{\rho} \approx \frac{1}{\omega'}, \qquad B' \gtrsim 0.1 \tag{3b}$$

Due to the threshold condition, the mean free path is constant above $\sim 4\times10^{12}$ G. Using Eqn (1), the approximate mean free path would be

$$\frac{\lambda_A}{\rho} \approx \frac{0.1}{\omega' B'}, \tag{4}$$

so that,

$$\frac{\lambda}{\lambda_A} \approx 1 + 210\, B'^{\,2.7}, \qquad B' \lesssim 0.1 \tag{5a}$$

$$10\, B', \qquad B' \gtrsim 0.1 \tag{5b}$$

The actual mean free paths of curvature radiation photons are therefore larger than those derived using the well known asymptotic limit and this discrepancy increases with field strength.

The longer mean free paths will cause the voltage drop at the polar cap to be somewhat higher than previously estimated[1,2] although this should not be a large effect. The secondary particle yields of the cascades above the acceleration region will be much more sensitive to changes in the mean free path because the multiplicative effects of large numbers of photons are involved. Longer mean free paths in a magnetic field which falls off with distance from the star should decrease the number of pairs produced per primary particle in these cascades. If proposed effects due to the vacuum index of refraction in a magnetic field are present, λ could be even larger.[8]

ORIGINAL PAGE IS
OF POOR QUALITY

DISCRETE e^+e^- PAIR STATES

When the pair is produced, the electron and positron must occupy discrete energy states with well defined energies perpendicular to the magnetic field. The spacing of these states in energy increases with B, reaching $\Delta E \sim mc^2$ at B_{cr}. For a given photon energy and field strength, there is a set of kinematically allowed states into which the pair can be produced. Figure 2 shows the number of these states as a function of photon energy and magnetic field for curvature radiation photons which are emitted parallel to B and travel one mean free path before producing the pair. At each magnetic field, the photon's energy must exceed a certain value before a pair can be produced with at least one member in an excited state. In fields $\gtrsim 5 \times 10^{12}$ G, a significant fraction of photons in the curvature radiation spectrum (for typical pulsar parameters) will produce pairs in the ground state.

Models of pulsar cascades[4] have shown that synchrotron radiation γ-rays from secondary particles are necessary to sustain a cascade with several photon generations and high pair yields. Curvature radiation from the pairs is much less efficient and unless

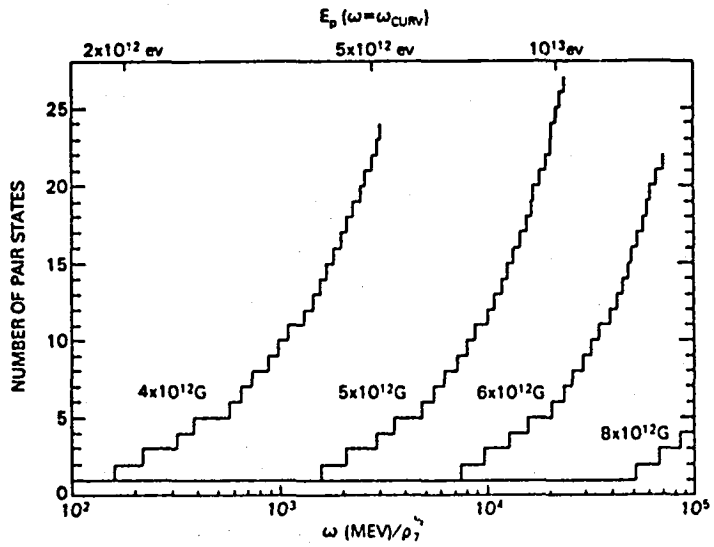

Fig. 2. Number of energetically allowed e^+e^- states vs. curvature radiation photon energy for different magnetic field strengths with constant radius of curvature, $\rho_7 \equiv \rho/10^7$ cm. The top scale is the primary particle energy E_p for which the critical energy $\omega_{curv} = (3/2)\ (E_p/mc^2)^3\ c/\rho = \omega$.

radii of curvature are significantly less than dipole, the cascade terminates after one photon generation. In magnetic fields high enough to suppress production of pairs in excited states, synchrotron radiation cannot take place (the photon energy is fed into particle motion parallel to the field). The efficiency of the cascades should therefore decrease rapidly above some field

ORIGINAL PAGE IS
OF POOR QUALITY

strength, depending on the critical frequency $\omega_{curv} = (3/2)(E_p/mc^2)^3 c/\rho$ of the primary particle curvature spectrum (Figure 3). Cascade efficiency (ie. the ratio of secondary to primary particles) will increase with field strength below this limit, however. For values of the primary particle energy E_p predicted by various acceleration models [1,2,3], copious pair production by cascades near the polar cap would not be expected to occur for field strengths above $B \sim 6\text{-}8 \times 10^{12}$ G.

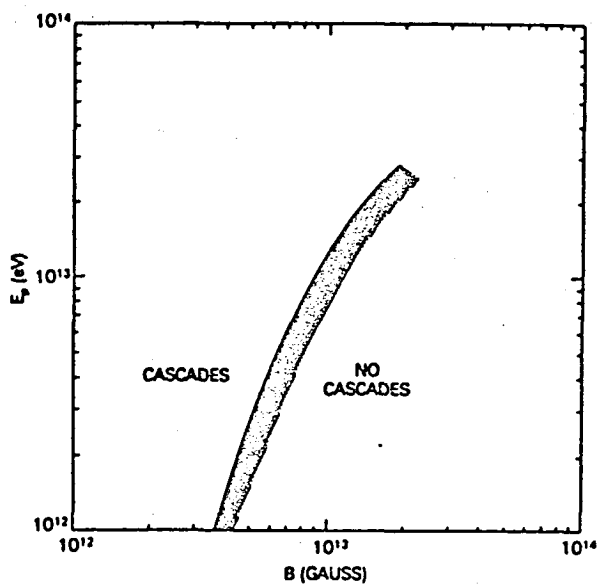

Fig. 3. Primary particle energy (i.e. polar cap acceleration voltage) vs. magnetic field strength above which all curvature radiation photons (with $\omega \lesssim 3\,\omega_{curv}$) produce pairs in the ground state.

CONCLUSIONS

This reevaluation of pair production by curvature radiation photons in pulsar magnetic fields has shown that threshold effects on the attenuation coefficient can have significant consequences for pair-photon cascades. In particular, there should be a maximum in the pair yield per primary particle as a function of magnetic field strength with the yields diminishing rapidly in fields $\gtrsim 6\times10^{12}$G where synchrotron radiation is suppressed. Since the copious production of e^+e^- pairs is necessary for coherent radio emission in most pulsar models, this may imply that there is a high magnetic field cutoff for radio pulsars.

REFERENCES

1. J. Arons and E. T. Scharlemann, Ap.J., 231, 854 (1979).
2. J. Arons, this proceeding (1983).
3. M. A. Ruderman and P. G. Sutherland, Ap.J., 196, 51 (1975).
4. J. K. Daugherty and A. K. Harding, Ap.J., 252, 337 (1982).
5. J. K. Daugherty and A. K. Harding, Ap.J., in press (1983).
6. J. K. Daugherty and A. K. Harding, this proceeding (1983).
7. T. Erber, Rev. Mod. Phys., 38, 626 (1966).
8. A. E. Shabad and V. V. Usov, Nature, 295, 215 (1982).

N83
27935

UNCLAS

ORIGINAL PAGE IS
OF POOR QUALITY

N83 27935

D7

e^+-e^- ANNIHILATION AND THE COSMIC X-RAY BACKGROUND

Demosthenes Kazanas and Richard Arrick Shafer
NASA/Goddard Space Flight Center
Greenbelt, MD. 20771
and
Department of Physics
University of Maryland

ABSTRACT

The possibility that the processes responsible for the Cosmic X-ray Background (CXB) would also produce an e^--e^+ annihilation feature is examined. Under the assumption that these processes are thermal, the absence of a strong e^--e^+ annihilation feature places constraints on the compactness (L/R ratio) of these sources. Observations favor sources of small compactness ratio.

INTRODUCTION

The fact that the X-ray sky is dominated by an isotropic component (the so called Cosmic X-ray Background, hereafter CXB) had been established by the earliest X-ray astronomy observations[1]. The subsequent satellite X-ray observations, especially by the A-2 and A-4 experiments on HEAO 1[2,3], allowed the detailed spectral determination of CXB. The observed spectrum in the region 3-150 keV, along with the higher energy data is shown in fig 1. The HEAO 1 experimenters have found that thermal bremsstrahlung from an optically thin plasma of temperature 40 ± 5 keV provides a remarkably good fit to the data from 3 to 100 keV. Interestingly enough, no studied population of sources is known to have a thermal spectrum with the required properties.

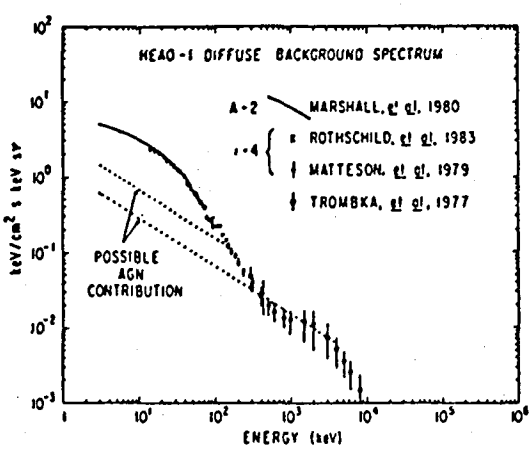

Fig. 1 - The unresolved X and gamma-ray background. (From refs [2,3,12,13])

One can of course contrive to combine sources with a variety of spectra emitting over a range of red shifts to produce the observed total background spectrum, even if the individual spectra are different than that of CXB[4]. The shape of of the spectrum however clearly suggests a thermal distribution of rather specific temperature and it would be more natural if the CXB could be

 PRECEDING PAGE BLANK NOT FILMED

ORIGINAL PAGE IS
OF POOR QUALITY

explained as such.

A thin thermal bremsstrahlung from a heated intergalactic medium will provide such a spectrum [5,6]. However, the energy required to heat a diffuse uniform medium to such a temperature is quite large. Also, the low densities and consequent long electron-ion coupling times provide difficulties in attaining and maintaining a Maxwellian distribution for the medium[7]. Clumping of the medium would reduce the input energy requirements and the coupling time scales. Taken to extremes, the clumps might be reduced to a size comparable to galaxies, or smaller, becoming "compact" sources of X-rays.

For either the heated intergalactic medium or the "compact source" models for the CXB, the bulk of the emission originates at redshifts ~ 2-3 (or even larger) so that the corresponding source temperature would be $kT \gtrsim 100$-200 keV. For these temperatures a sufficiently compact source will produce electron-positron pairs from the tails of the photon and particle thermal distributions. Under certain conditions the positron abundance would be sufficient to produce an observable e^+-e^- annihilation feature in the CXB.

THE POSITRON ABUNDANCE

In a thermal plasma of temperature $kT \gtrsim 100$ keV it is possible to produce positrons at significant abundances by ee, $e\gamma$ or $\gamma\gamma$ collisions since a non-negligible fraction of the particles and photons at the tails of the distributions fulfills the pair production threshold condition. Their steady state abundance is determined by the balance between pair production and annihilation reactions (for a detailed treatment see ref. 8).

In the cases of interest for the CXB the dominant positron production is due to $\gamma\gamma$ reactions so the ee, $e\gamma$ reactions will not be considered further . (Their cross sections are correspondingly smaller by α^2 and α). The approximate expressions for the production and annihilation the rates are:

$$R_{\gamma\gamma} = \frac{3}{16\pi}\,\sigma_T c\, K_\gamma^{\,2}\, f(x)\ , \qquad (1)$$

$$R_{+-} = \frac{3}{8}\,\sigma_T\ c\ \ \eta_+\eta_-\ .$$

where η_+, η_-, are the positron and electron number densities, σ_T the Thomson cross section and $x = 2\, m_e c^2/kT$. $f(x)$ is a function of the temperature only, resulting from the averaging of the photon-photon pair production reaction rate over the photon distribution functions. It is given by

$$f(x) = c_1\,\frac{e^{-x}}{x(x+c_2)},$$

where $c_1 = 1.143$ and $c_2 = 3.63$ are constants. K_γ is the normalization

ORIGINAL PAGE IS
OF POOR QUALITY

of the bremsstrahlung photon distribution function determined by the condition

$$\int_0^\infty \frac{K_\gamma}{E} e^{-E/kT} E \, dE = \frac{L(1+\tau)}{\pi R^2 c} \text{ or}$$

$$K_\gamma = \frac{L(1+\tau)}{kT \pi R^2 c} \quad . \tag{2}$$

where L, R, τ, T are respectively the luminosity, radius, optical depth and temperature of the sources. The steady state condition $R_{\gamma\gamma} = R_{+-}$ gives

$$\frac{1}{2\pi} \left(\frac{K_\gamma}{n_+ + n_-}\right)^2 f(x) = \frac{n_+ n_-}{(n_+ + n_-)^2} \; . \tag{3}$$

Since the compact sources presently considered are presumably gravitationally bound, one can scale L and R by their gravitational units i.e. the Eddington luminosity ($L_E = 10^{38}$ M erg s^{-1}) and the Schwarzschild radius ($R_s = 3\ 10^5$ M cm) where M is the mass of the sources in solar masses. For this we introduce two parameters F and f, both with expected values between 0 and 1, defined as

$$F \equiv L/L_E \text{ and } f \equiv R_s/R \; .$$

Their product $Ff = L/R$ is a mass independent measure of their compactness. A high value of Ff corresponds to a high density of photons and hence e^+e^- pairs. The additional factor of R in K_γ can be expressed in terms of the optical depth τ, since $(n_+ + n_-)\, \sigma_T R = s\tau$ where s is the aspect ratio of the source, i.e. the ratio of its largest to its shortest dimension. We can therefore reexpress eq (3) in terms of the positron abundance $\lambda \equiv n_+/n_-$ by:

$$2\times10^3 \, Ff \, e^{-x/2} \left(\frac{x}{x+c_2}\right)^{1/2} \frac{\tau+1}{s\tau} = \frac{\lambda^{1/2}}{1+\lambda} \; . \tag{4}$$

COMPARISON TO OBSERVATION

Equation (4) can be directly related to observations of the CXB. Let A be the ratio of the annihilation to the bremsstrahlung spectral luminosity at the peak energy of the annihilation feature, $E = m_e + kT$. Since no obvious annihilation feature is observed in the CXB $A \lesssim 1$. Using the results of ref. 9, one can relate λ to A and x by

$$\frac{\lambda^{1/2}}{1+\lambda} \lesssim 0.134 \, A^{1/2} \, x^{-1/4} \, e^{-x/4} \; . \tag{5}$$

Elimination of λ between (4) and (5) gives

$$Ff \lesssim 1.7 \; 10^{-4} \, e^{x/4} \, \frac{(x+c_2)^{1/2}}{x^{1/4}} \, A^{1/2} \, \frac{sx}{\tau+1} \; . \tag{6}$$

ORIGINAL PAGE IS
OF POOR QUALITY

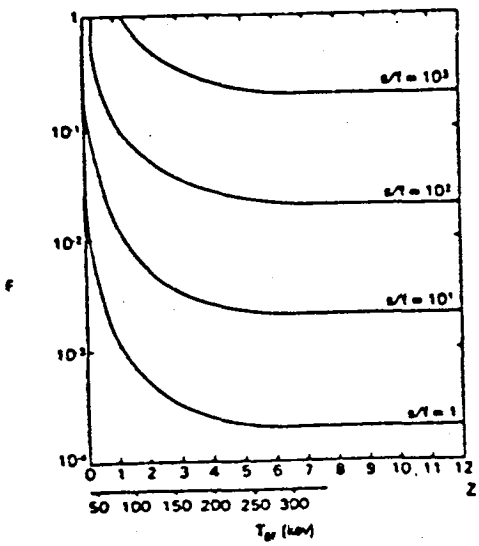

Fig. 2. Limits on source luminosity F (in units of L_E) vbs redshift of CXB production, z, for different source effective sizes, s/f (in units of R_s). The temperature is the source temperature in the emmitter frame.

Eq (6) is independent of the mass of the sources and limits (as a function of the redshift Z at which the CXB was produced) their L/R ratio to be compatible with the absence of a prominent annihilation feature in the CXB. The optical depth τ of the sources is unknown, however it is constrainted to be $\tau \lesssim 3$ otherwise the corresponding self-Comptonization Wien peak should be apparent in the spectrum[10]. Another unknown parameter of the sources is the aspect ratio. For spherical sources s= 1, although it could be s>>1 for sources of thin disk geometry. It appears, however, s = 1 that for sources emiting close to their Eddington luminosity[11]. The constraints imposed by eq (6) are shown in fig 2. For example, the absence of a prominent annihilation feature at 100-150 keV, constraints compact sources (f≈0.1) operating at z≈4 to emit at a small fraction of their Eddington luminosity. Due to the absence of positive detection of such feature all the derived constraints are in form of inequalities which however may prove important in understanding the nature of the sources of CXB. Fig 3 shows the superposition of the energy spectrum of thermal bremsstrahlung with T = 200 keV and an annihilation feature of the same temperature and A = 1. Such a feature appears detectable, though unfortunately in this example it peaks in the observer frame energy range E $\gtrsim$ 100 keV, which is probably dominated not by the thermal component but by the contribution of active galaxies. This is currently very poorly known and we may always have to be content with the existing upper limts. A positive detection an annihilation feature in the CXB spectrum, rather than the above qualitative upper bound, would provide an important contribution to the understanding of the CXB's origin. Such a detection will determine precisely the emitter-frame temperature (and hence the redshift) of the sources, it will signify that they are compact and it will provide a consistency check for the temperature of the termal component. If this feature is not detectable in the CXB spectrum, as a whole it may someday be studied

ORIGINAL PAGE IS
OF POOR QUALITY

in individual spectra of compact objects, if such objects make up the background. However such studies will probably require high energy imaging capabilities beyond those planned for the next generation of experiments.

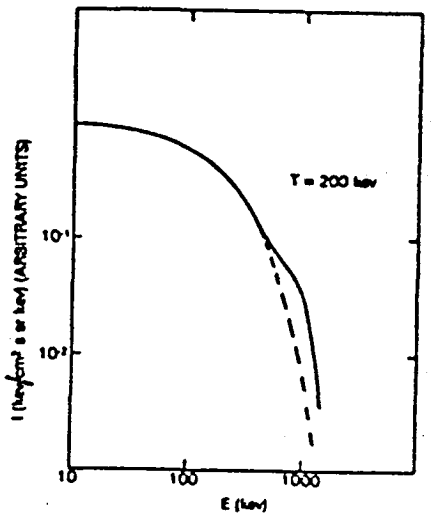

Fig. 3. Superposition of bremsstrahlung and annihilation radiation energy spectrum for A = 1 and T = 200 keV.

REFERENCES

1. R. Giacconi, J. Gursky, F. Paolini, B. Rossi, Phys. Rev. Lett., 9, 439 (1962).
2. F. E. Marshall, E. A. Boldt, S. Holt, R. Miller, R. F. Mushotzky, L. A. Rose, R. E. Rothschild and P. Serlemitsos, Ap. J., 235, 377 (1980).
3. R. E. Rothschild, R. F. Mushotzky, W. A. Baity, D. E. Gruber and J. L. Matteson, Ap.J., (1983) (in press).
4. G. DeZotti, E. A. Boldt, A. Cavaliere, L. Danese, A. Francischini, F. E. Marshall, J. H. Swank and A. J. Szymkoviak, Ap. J., 253, 47 (1982).
5. R. Cowsik and E. J. Kobetich, Ap.J., 177, 585 (1972).
6. G. B. Field and S. Perrenod, Ap.J., 215, 717 (1977).
7. A. C. Fabian and A. K. Kembhavi, in Heeschen and Wade (eds.) IAU Symposium 97 on Extragalactic Radio Sources, (Reidel; Dordrecht, 1982) p. 453.
8. R. Svensson, Ap.J., 258, 335 (1982).
9. R. Ramaty and P. Meszaros, Ap.J., 250, 384 (1981).
10. A. D. Lightman and D. L. Band, Ap. J., 251, 715 (1981).
11. J. Eilek, Ap.J., 236, 664 (1980).
12. J. L. Matteson, D. E. Gruber, P. L. Nolan, L. E. Peterson and R. L. Kinzer, BAAS, 11, 653 (1979).
13. J. I. Trombka, C. S. Dyer, L. G. Evans, M. J. Bielfeld, S. M. Seltzer and A. E. Metzger, Ap.J., 212, 925 (1977).

N83
27936

UNCLAS

ORIGINAL PAGE IS
OF POOR QUALITY

N83 27936

D8

THE ORIGIN OF THE GALACTIC CENTER ANNIHILATION RADIATION

R.E. Lingenfelter
Center for Astrophysics & Space Sciences, C-011
University of California, La Jolla, CA 92093 USA

R. Ramaty
Laboratory for High Energy Astrophysics
NASA/Goddard Space Flight Center, Greenbelt, MD 20771 USA

ABSTRACT

Observations of the e^+-e^- annihilation radiation from the Galatic Center suggest that something truly extraordinary is occurring there. We review the observations of this intense, time-varying, 0.511 MeV emission and discuss the implications of these and other recent observations on the positron production process, the annihilation region and the fundamental nature of the Galactic Center source.

INTRODUCTION

A year ago we reviewed[1] the possible origins of the e^+-e^- annihilation radiation from the Galactic Center and concluded that the most likely process for producing the annihilating positrons is photon-photon pair production in the vicinity of a massive black hole at the center of our Galaxy. We briefly summarize here the evidence and arguments leading to this conclusion, and at the same time discuss the implications of new observations and calculations that shed further light on the problem.

We briefly summarize the observations[2] and then discuss in turn their implications on the nature of the annihilation region, the positron production process and the Galactic Center source itself.

OBSERVATIONS

Intense positron annihilation radiation at 0.511 MeV has been observed from the direction of the Galactic Center for over a decade. This emission was first seen in a series of balloon observations[3–5] with low-resolution NaI detectors starting in 1970. But it was not until 1977 that the annihilation line energy of 0.511 MeV was clearly identified with high-resolution Ge detectors flown by Leventhal, MacCallum and Stang[6]. The latter observation also revealed that the line is very narrow (FWHM $\lesssim$ 3.2 keV) and suggested that the continuum below 0.511 MeV may include a significant contribution from three-photon positronium annihilation, consistent with $\sim$ 90% of the positron annihilation taking place through positronium formation.

The existence of this very narrow line was confirmed by Riegler et al.[7] with Ge detectors on HEAO-3 in the fall of 1979. These observations set an even more stringent limit on the line width (FWHM < 2.5 KeV) and determined the line center energy as 510.90 ± 0.25 keV.

The HEAO-3 observations[7] also provided new information on the location and spacial extent of the emission region and most important showed that the line intensity varies significantly in time. In particular, these observations showed that the line emitting region is smaller than the angular resolution of the detector (35° FWHM) and that the direction of the source coincides with that of the Galactic Center, within the observational uncertainty of ± 4°. Moreover the observations showed that the 0.511 MeV line intensity decreased by a factor of three in six months, from $(1.85 \pm .21) \times 10^{-3}$ photons/cm^2 sec in the fall of 1979 to $(0.65 \pm .27) \times 10^{-3}$ photons/cm^2 sec in the spring of 1980. This variability has

PRECEDING PAGE BLANK NOT FILMED

ORIGINAL PAGE IS
OF POOR QUALITY

been confirmed by balloon-borne Ge detector observations[8-9]. Observations[10] with a NaI detector in the fall of 1977 could also indicate a variation on a time scale as short as 10 days, but it seems much more likely that the higher 0.511 MeV intensity observed with this detector results from a larger diffuse galactic component seen in its much greater (100° FWHM) field of view.

Observations of continuum emission in the hard X-ray and gamma-ray bands have recently been reviewed by Matteson[11]. The hard X-ray emission is also time variable and is weakly correlated with the variability of the 0.511 MeV line (e.g. Ref. 9). These observations set an upper bound of 2×10^{33} erg/sec on the Galactic Center continuum luminosity at photon energies $> m_e c^2$, since only part of this emission may come from the same source as the annihilation radiation.

The luminosity of the Galactic Center region at various photon energies, implied by these and other observations are summarized in Figure 1 from Reference 1.

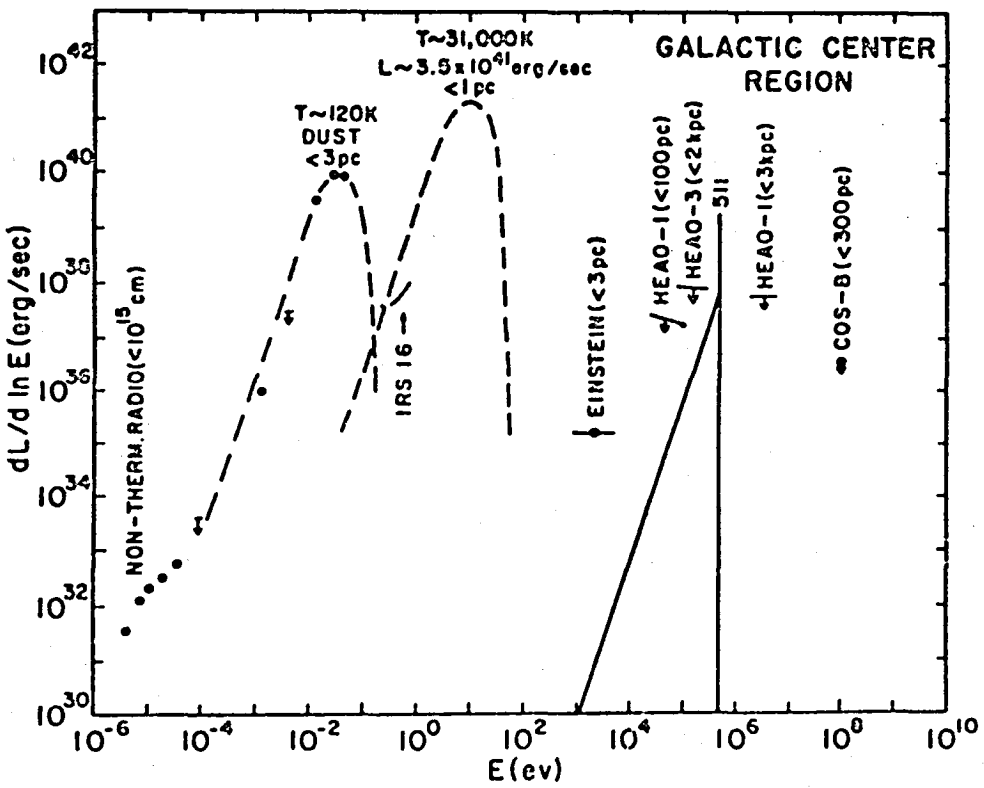

Figure 1. The luminosity per unit lnE as a function of photon energy, E, from the region around the Galactic Center. Data are shown for the compact ($< 10^{15}$ cm) nonthermal radio source[12], the ~ 3pc dust ring[13], the nonthermal infrared source IRS 16 (Ref. 14), the soft X-ray emission (< 3pc) from the EINSTEIN satellite measurements[15], the hard X-ray emission from HEAO-1 (Ref. 11), the 511 KeV line and positronium continuum[6,7], and the gamma ray emission from HEAO-1 (Ref. 11) and COS-B (Ref. 16). Also shown as dashed curves are the blackbody luminosity at ~ 31,000 K required[17] to account for ionization in the warm IR clouds within < 1pc of the Galactic Center and a blackbody luminosity at 120 K as inferred[13] from the far infrared observations of the ~ 3pc dust ring.

ORIGINAL PAGE IS
OF POOR QUALITY

THE ANNIHILATION REGION

The nature of the positron annihilation region is constrained by the intensity variations, the line width and the line center energy. The size of the region should not exceed about 10^{18} cm, the distance traveled by relativistic positrons in 1/2 year. The density of the gas in which the positrons annihilate should be larger than 10^5 H/cm^3, the minimum density required to slow them down in 1/2 year, but less than 10^{15} H/cm^3 in order not to break up the triplet positronium before it annihilates. Since triplet positronium could also be broken up (R. McCray, private communication) by photons of energy > 6.8 eV, the energy density of such photons should not exceed $\sim 10^3$ erg/cm^3 in the annihilation region, or if the 31,000 K emission[17] (Fig. 1) comes from a single source the annihilation region must be $> 2 \times 10^{13}$ cm away from it, assuming a positronium ionization cross section of 3×10^{-18} cm^2.

The observed line width requires[18] that this gas also be at least partially ionized ($n_e < 0.1n$). If the gas were neutral, the line width would be larger than observed because it would be Doppler broadened, not by the thermal motion of the gas, but by the velocity of energetic positrons forming positronium in flight by charge exchange with neutral hydrogen. In a partially ionized gas, however, positrons lose energy to the plasma fast enough that the positrons thermalize before they annihilate or form positronium. The line width thus reflects the temperature of the medium, so that the observations require a temperature $\lesssim 5 \times 10^4$ K. The line width further limits any velocities of rotation, expansion or random motion to < 700 km/sec, while the line center energy implies a bulk velocity along with line of sight $-90 < v < +200$ km/sec and a gravitational redshift $z < 7 \times 10^4$.

The strongest of these constraints are summarized in Table I.

Table I

CONSTRAINTS ON THE e^+-e^- ANNIHILATION REGION AT THE GALACTIC CENTER

Physical Parameter	Constraint	Observation
Size	$< 10^{18}$ cm	variability
Gas density	$> 10^5$ H/cm^3	variability
Ionization state	$n_e/n > 0.1$	line width
Temperature	$\lesssim 5 \times 10^4$ K	line width
Rotation, expansion or random motion	< 700 km/sec	line width
Bulk motion along line of sight	$-90 < v < +200$ km/sec	line center energy
Gravitational redshift	$z < 7 \times 10^4$	line center energy

As we previously suggested[19] possible annihilation sites which satisfy these constraints are the warm clouds[17] and the compact source IRS 16 (Ref. 12), observed within the central parsec of the Galaxy.

THE POSITRON SOURCE

The nature of the positron source is also strongly constrained by the observed variation of the 0.511 MeV intensity and by observations at other wavelengths. The decrease of a factor of three in the line intensity in six months clearly excludes any of the multiple, extended sources, such as cosmic rays, pulsars[20], supernovae[21], or primordial black holes[22], previous proposed. Instead, it essentially requires a single, compact ($< 10^{18}$ cm) source which is apparently located either at, or close to, the Galactic Center and which is inherently variable on time scales of six months or less.

ORIGINAL PAGE IS
OF POOR QUALITY

The observed 0.511 MeV line intensity of $\sim 2 \times 10^{-3}$ photons/cm^2 sec requires at the distance of the Galactic Center ($\sim$ 10 kpc) a positron annihilation rate of 4×10^{43} e^+/sec, if $\sim$ 90% of the positrons annihilate via positronium. This rate corresponds to minimum luminosity of $\sim 6 \times 10^{37}$ erg/sec in both the line and three-photon continuum. With such a luminosity the Galactic Center is the most luminous gamma-ray source in the galaxy. The uniqueness of this source makes it unlikely that it results from the chance occurrence of the youngest supernova or pulsar along with line of sight to the center of the galaxy.

The strongest constraints on the various positron production processes are set[1] by observations of continuum emission at energies $> m_ec^2$ from the direction of the Galactic Center[11]. When compared with the annihilation radiation luminosity, the continuum gamma ray luminosity implies a very efficient positron production process, one in which more than 30% of the total radiated energy $> m_ec^2$ goes into electron-positron pairs. If the positron production occurs on time scales comparable to that of the observed variation and in an essentially optical thin region which emits isotropically, only photon-photon pair production can provide the required high efficiency.

We considered[1] two geometries for the positron production region: a spherical volume in which e^+–e^- pairs are produced by photons interacting isotropically and a beam in which the pairs are produced by photon interactions only at small angles.

The most efficient pair production occurs in isotropic interactions of photons at energies close to m_ec^2. The pair production rate Q in a spherical source of radius r may be approximated by

$$Q \sim \tfrac{1}{2}\, n_\gamma^2 \langle \sigma c \rangle \frac{4\pi}{3} r^3$$

where $\langle \sigma c \rangle$ is the average pair production cross section times the velocity of light, equal to $\sim 3 \times 10^{-15}$ cm^3/sec for black body photons of temperature $\sim m_ec^2$, and n_γ is the photon number density. Assuming that the source is optically thin, the photon density can also be related to the continuum luminosity at energies $\gtrsim m_ec^2$ by

$$L \sim \frac{\epsilon n_\gamma c 4\pi r^2}{3},$$

where ϵ is the average photon energy and r/c is the photon residence time. Combining these two equations and setting $\epsilon \sim m_ec^2$, we see that for a given continuum luminosity the positron production rate depends only on the source size, such that the radius,

$$r \sim \frac{3 \langle \sigma c \rangle}{8\pi c^2 (m_ec^2)^2} \frac{L^2}{Q} \sim 6\times10^{-25} \frac{L^2}{Q} \text{ (cm)}.$$

From the observed luminosity limit of $L \lesssim 21 \times 10^{38}$ erg/sec and a production rate Q equal to the annihilation rate of 4×10^{43} e^+/sec, the radius of the positron source must be $\lesssim 6 \times 10^8$ cm.

Pair production by isotropic photon-photon interactions thus requires an exceedingly compact course, but with a high luminosity. The most obvious candidate is a blackhole. But if this source is a blackhole releasing gravitational energy of accreting matter close to its Schwarzschild radius, then it must have a mass $< 10^3$ $M_\odot$, which is much smaller than the masses of 10^6 to 10^7 $M_\odot$ blackholes that have been suggested[17,23] at the Galactic Center. Yet such a small size would be consistent with arguments by Ozernoy[24] that the Galactic Center cannot contain a blackhole larger than about 10^2 $M_\odot$, if tidal disruption of stars is the principal source of the accreting matter on which it grows.

The photons needed to produce the pairs could themselves be produced in a hot accretion disk around the blackhole[25]. A luminosity of $\sim 2 \times 10^{38}$ erg/sec requires an accretion rate of $\sim 3 \times 10^{-8}$ $M_\odot$/yr which would form a $\sim$ 300 $M_\odot$ hole in the age of the Galaxy. A major fraction of the $e^\pm$ pairs produced by photon-photon collisions above the

ORIGINAL PAGE IS
OF POOR QUALITY

disk could then escape from the source region before they annihilate, a constraint (Table 1) set by the absence of any measurable redshift in the energy of the annihilation line.

We turn now to the alternative geometry of pair production by small angle photon interactions in a beam, which may be produced[25,27] by dynamo action in a magnetic field accreting onto a blackhole. We previously showed[1] that with a beam the constraint on the size of the production region could be greatly relaxed, but at the expense of a much higher beam luminosity in gamma rays of energy $>> m_e c^2$. This possibility for producing positrons in the Galactic Center was first suggested by M. Burns (private communication 1982) and differs from Novikov's[22] model (in this volume), which relies on the relatively less efficient production by beam photons interacting with gas in a cloud.

The pair production rate Q for small angle ($\theta \sim r_b/l$) photon interactions in a beam of radius r_b and length l may be approximated by

$$Q \sim \tfrac{1}{2}\, n_\gamma^2 \langle \sigma v_\perp \rangle\, \pi r_b^2 l,$$

where $v_\perp \sim (r_b/l)c$ is the mean transverse velocity of the interacting photons, and n_γ is the density of those photons with energies greater than the small angle pair production threshold $E_{th} \sim (l/r_b)\, m_e c^2$. This density can be related to the beam luminosity of such photons by

$$L_b \sim (l/r_b)\, m_e c^2\, n_\gamma c\, \pi r_b^2.$$

Combining these two equations, we see that the beam radius is

$$r_b \sim \frac{\langle \sigma c \rangle}{2\pi c^2 (m_e c^2)^2} \frac{L_b^2}{Q} \left(\frac{r_b}{l}\right)^2 \sim 8 \times 10^{-25} \frac{L_b^2}{Q} \left(\frac{r_b}{l}\right)^2 \text{cm}.$$

Thus for a pair production rate Q of 4×10^{43} e^+/sec the beam radius could be as big as $\sim 10^{12}$ cm, or equal to the Schwarzschild radius of a 3×10^6 $M_\odot$ blackhole, if the beam luminosity at photon energies greater than 25 MeV were as high as half the Galactic Center bolometric luminosity limit of $\sim 3.5 \times 10^{41}$ erg/sec, and the aspect ratio of the beam were 0.02, corresponding to angle of 1°.

The resulting pairs would also have energies of $\sim$ 25 MeV, comparable to those of the photons which produced them. But they could be stopped and annihilate to give narrow 0.511 MeV line emission, if the beam hit a gas cloud. The bulk of the pair energy, amounting to $\sim 10^{40}$ erg/sec, would be dissipated in heating the gas which could in turn reradiate it isotropically as thermal radiation consistent with the constraints on the $\lesssim$ 30,000 K luminosity. Since the radiation yield of $\sim$ 25 MeV electrons and positrons is $\lesssim$ 3%, their bremsstrahlung could also be consistent with the hard X-ray and gamma-ray luminosity limit of $\lesssim 2 \times 10^{38}$ erg/sec.

The detailed energetics of both of these geometries, however, are still under study.

SUMMARY

The observed time variations and line width of the e^+–e^- annihilation radiation from the Galactic Center require that the positrons be produced essentially by a single source and that they annihilate in an ambient gas of density $> 10^5$ H/cm^3, ionization fraction > 10%, temperature $< 5 \times 10^4$ K, and confined to a region of size $< 10^{18}$ cm. Such conditions may exist in the warm clouds and the compact source IRS 16 within the central parsec of the galaxy.

The limits on the accompanying continuum emission at energies $> m_e c^2$ set strong constraints on the positron production process, requiring an exceedingly high efficiency, such that > 30% of the total radiated energy $> m_e c^2$ goes into e^+–e^- pairs. The most likely mechanism appears to be pair production in photon-photon collisions in the close vicinity of a massive blackhole, either near the hot ($kT \sim m_e c^2$) inner part of an accretion disk around a $\sim 10^2$ $M_\odot$ blackhole, or in a beam of $\sim$ 25 MeV photons produced by a

ORIGINAL PAGE IS
OF POOR QUALITY

$\sim 10^6 M_\odot$ hole. In either case the absence of any measurable redshift in the line center energy requires that a large fraction of the positrons escape from the central source and annihilate at great distances from the hole ($> 10^3$ times the Schwarzschild radius).

ACKNOWLEDGEMENTS

The work of R.E.L. was supported by NASA grant NSG-7541.

REFERENCES

1. R.E. Lingenfelter and R. Ramaty, The Galactic Center (Am. Inst. Physics, New York, 1982), p. 148.
2. C.J. MacCallum and M. Leventhal, these proceedings (1983).
3. W.N. Johnson, F.R. Harnden and R.C. Haymes, Ap. J., *172* L1 (1972).
4. W.N. Johnson and R.C. Haymes, Ap. J., *184*, 103 (1973).
5. R.C. Haymes et al., Ap. J., *201*, 593 (1975).
6. M. Leventhal, C.J. MacCallum and P.D. Stang, Ap. J., *225*, L11 (1978).
7. G.R. Riegler et al., Ap. J., *248*, L13 (1981).
8. M. Leventhal et al., Ap. J., *260*, L1 (1982).
9. W.S. Paciesas et al., Ap. J. *260*, L7 (1982).
10. B.M. Gardner et al., The Galactic Center (Am. Inst. Physics, New York, 1982), p. 144.
11. J.L. Matteson, The Galactic Center (Am. Inst. Physics, New York, 1982), p. 109.
12. K.Y. Lo et al., Ap. J., *249*, 504 (1981).
13. I. Gatley, The Galactic Center (Am. Inst. Physics, New York, 1982), p. 25.
14. E.E. Becklin et al., Ap. J., *219*, 121 (1978).
15. M.G. Watson et al., Ap. J., *250*, 142 (1981).
16. B.N. Swanenburg et al., Ap. J., *243*, L69 (1981).
17. J.H. Lacy et al., Ap. J., *241*, 132 (1980).
18. R.W. Bussard, R. Ramaty and R.J. Drachman, Ap. J., *228*, 928 (1979).
19. R. Ramaty and R.E. Lingenfelter, Phil. Trans. R. Soc. Lond., *A301*, 671 (1981).
20. P.A. Sturrock and K.B. Baker, Ap. J., *234*, 612 (1979).
21. R. Ramaty and R.E. Lingenfelter, Nature, *278*, 127 (1979).
22. P.N. Okeke and M.J. Rees, A. Ap., *81*, 263 (1980).
23. D. Lynden-Bell and M.J. Rees, M.N.R.A.S., *152*, 461 (1971).
24. L.M. Ozernoy, Large Scale Characteristics of the Galaxy (Reidel, Dordrecht, 1979), p. 395.
25. D.M. Eardley et al., Ap. J., *224*, 53 (1978).
26. R.D. Blandford, Active Galactic Nuclei (Cambridge Univ. Press, London, 1979), p. 241.
27. R.V.E. Lovelace, J. McAuslan and M. Burns, Particle Acceleration Mechanisms in Astrophysics (Am. Inst. Physics, New York, 1979), p. 399.
28. N.S. Kardashev, I.D. Novikov, A.G. Polnarev and B.E. Stern, these proceedings (1983).

N83
27937

UNCLAS

N83 27937

CRITERIA FOR GRASAR ACTION IN ASTROPHYSICAL SOURCES

J. M. McKinley* and R. Ramaty
Laboratory for High Energy Astrophysics
NASA/Goddard Space Flight Center
Greenbelt, Maryland 20771

ORIGINAL PAGE IS
OF POOR QUALITY

ABSTRACT

The theory of gamma-ray amplification through stimulated annihilation radiation (grasar) was developed by Ramaty, McKinley and Jones[1] (hereafter RMJ). For gamma-ray bursts similar to the March 5, 1979 burst, an observed annihilation line of width <0.03 MeV would imply a grasar source. The minimum pair density needed for the onset of grasar action is $\sim 10^{30}$ cm^{-3} and the peak of the grasar line, without a gravitational redshift, is at < 0.5 MeV.

INTRODUCTION

An emission line at ~0.43 MeV, generally believed to be spontaneous, optically thin and gravitationally redshifted e^+-e^- annihilation, has been observed[2,3] from several gamma-ray bursts. The measured photon fluxes and the likely distances and sizes of the burst sources suggest[4], however, that for at least some bursts the source regions are optically thick. Compton scattering and γ-γ pair production are the principal mechanisms that would remove photons from an emission line in a gamma-ray burst source.

In a detailed calculation of the emissivities and the absorption coefficients for two-photon pair production and annihilation and the accompanying Compton and inverse Compton scattering, RMJ[1] showed that an emission line at ~0.43 MeV could be produced in an optically thick source without a gravitational redshift by amplified annihilation radiation. In the present paper we consider the observational signatures that would imply the existence of such a grasar source, the minimum e^+-e^- pair density needed for the onset of grasar action and the reasons that the central energy of the two-photon grasar line is at < 0.5 MeV.

OBSERVATIONAL REQUIREMENTS FOR A GRASAR SOURCE

The need for a grasar source can be seen from a relationship between the width of an observed annihilation line, ΔE, the fluence in the line, F, the duration of the emission of the line photons, Δt, the source distance, d, and the source projected area, A. We derive this relationship by comparing the minimum pair density required to produce the line by nonamplified radiation (i.e. radiation with total absorption coefficient $K_T>0$) with the maximum pair density allowed by broadening due to pair degeneracy[1] and the

*Also at Physics Department, University of Maryland, College Park

ORIGINAL PAGE IS
OF POOR QUALITY

observed upper limit on the line width. We first calculate the minimum pair density.

The equation of radiative transfer, $dI/d\ell = j - K_T I$, requires that for nonamplified annihilation radiation, the ratio of the spontaneous annihilation emissivity to the absorption coefficient, j/K_T, be larger than the radiation intensity I. Otherwise $dI/d\ell<0$ and no observable radiation is produced. RHJ[1] carried out detailed calculation of j and K_T for pair plasmas in a bath of ambient photons. Here we estimate the annihilation emissivity, j, by a simple expression which is consistent with their calculations,

$$j \approx 2\pi r_o^2 c\, n_\pm^2/(4\pi\Delta E), \tag{1}$$

where $n_\pm$ is the pair density (we assume equal positron and electron densities) and $r_o=2.82\times10^{-13}$ cm. To calculate the minimum pair density, we can ignore the ambient photons. Thus $K_T \approx K_C$, where

$$K_C \approx 2n_\pm \pi r_o^2 \tag{2}$$

is the Compton absorption coefficient. The intensity is given by

$$I = \frac{d^2F}{A\Delta t\Delta E} \quad . \tag{3}$$

By combining Eqs. (1), (2) and (3) and using the condition for observable nonamplified radiation ($j/K_T>I$) we obtain

$$n_\pm > \frac{4\pi d^2 F}{A\Delta t c} \approx (4\times10^{23}\ \mathrm{cm}^{-3})\left(\frac{d}{1\mathrm{kpc}}\right)^2\left(\frac{F}{1\ \mathrm{ph\ cm}^{-2}}\right)\left(\frac{A}{1\mathrm{km}^2}\right)^{-1}\left(\frac{\Delta t}{1\mathrm{sec}}\right)^{-1} . \tag{5}$$

We next consider the upper limit on $n_\pm$. For nonamplified annihilation, degeneracy broadening[1] sets a lower limit on the width of the annihilation line,

$$\Delta E > 0.8\, p_F c = 0.8(3\pi^2)^{1/3}\hbar c\, n_\pm^{1/3}, \tag{6}$$

where p_F is the Fermi momentum of the pairs. An observed line width or upper limit on the width, therefore, sets an upper limit on $n_\pm$,

$$n_\pm < 8.5\times10^{27}\ \mathrm{cm}^{-3}\ (\Delta E/0.1\mathrm{MeV})^3. \tag{7}$$

By combining Eqs. (5) and (7) we obtain a necessary condition for the production of an observed line by nonamplified annihilation,

$$\left(\frac{A}{1\mathrm{km}^2}\right)\left(\frac{\Delta t}{1\mathrm{sec}}\right) > 4.7\times10^{-5}\left(\frac{F}{1\ \mathrm{ph\ cm}^{-2}}\right)\left(\frac{d}{1\mathrm{kpc}}\right)^2\left(\frac{\Delta E}{0.1\mathrm{MeV}}\right)^{-3}. \tag{8}$$

The most intense astrophysical annihilation line observed so far is that seen[2] in the spectrum of the 1979, March 5 burst whose source direction coincides[5] with that of the supernova remnant N49

ORIGINAL PAGE IS
OF POOR QUALITY

in the Large Magellanic Cloud (LMC). For this burst[2] $F \sim 7$ photons cm^{-2}, $\Delta E < 0.13$ MeV, and if the line-formation time equals the duration of the impulsive phase, $\Delta t \sim 0.15$ sec. Furthermore, if the source of the burst is indeed in the LMC, $d = 55$ kpc. Then from Eq. (8), nonamplified annihilation requires that $A > 3$ km^2. This condition can be satisfied on a neutron star surface since its projected area is ~ 300 km^2.

For the March 5, 1979 burst, however, both Δt and ΔE could have been significantly smaller than the values given above. In particular, the line formation time could be less than the total impulsive phase duration, since the annihilation time of the pairs is extremely short[6] ($\sim 10^{-15}$ sec). If future observations should indicate short durations and narrow lines, a strong case would exist for grasar sources in astrophysics.

THRESHOLD DENSITY FOR GRASAR ACTION

Spontaneous pair annihilation into two photons and the inverse process of two-photon pair production are necessarily accompanied by stimulated annihilation (e.g. Ref. 1). The absorption coefficient due to stimulated annihilation, K_{SA}, is always negative, but the generation of amplified annihilation radiation (i.e. grasar action) requires that the total absorption coefficient be negative for at least some photon energies,

$$0 > K_T = K_C + K_{pp} + K_{SA} \quad . \tag{9}$$

Here K_{pp} is contributed by pair production. K_{SA} is related[1] to the spontaneous emissivity of annihilation photons, j,

$$-K_{SA} = \frac{4\pi^3(\hbar c)^3}{cE^2}\, j, \tag{10}$$

where E is the photon energy. This expression, like its analogue for any other radiative process, can also be found directly from the Einstein A and B coefficients.

RMJ showed[1] that for grasar action to occur the pair density $n_\pm$ must exceed a threshold value. To provide an estimate of this threshold, we consider the case of a cold pair plasma ($kT \ll$ Fermi energy) with no ambient photons present. Such a degenerate system has the lowest threshold density, since $K_{pp}=0$ and K_C is reduced by the degeneracy. In this case we can use Eqs. (1), (2), (6) and (10) and $E = mc^2$ to obtain

$$-\frac{K_{SA}}{K_C} = 1.25\,\frac{\pi^{4/3}}{3^{1/3}}\left(\frac{\hbar}{mc}\right)^2 n_\pm^{2/3}\, f^{-1} = 5.9\times10^{-21}\left(\frac{n_\pm}{1\,cm^{-3}}\right)^{2/3} f^{-1}, \tag{11}$$

where f is the fraction of the degenerate positrons and electrons which can contribute to Compton scattering at the photon energy of interest. The threshold for grasar action occurs when $-K_{SA} = K_C$,

ORIGINAL PAGE IS
OF POOR QUALITY

i.e. at a pair density

$$n_{\pm} = 2.2 \times 10^{30}\ \mathrm{cm}^{-3}\ f^{3/2}. \qquad (12)$$

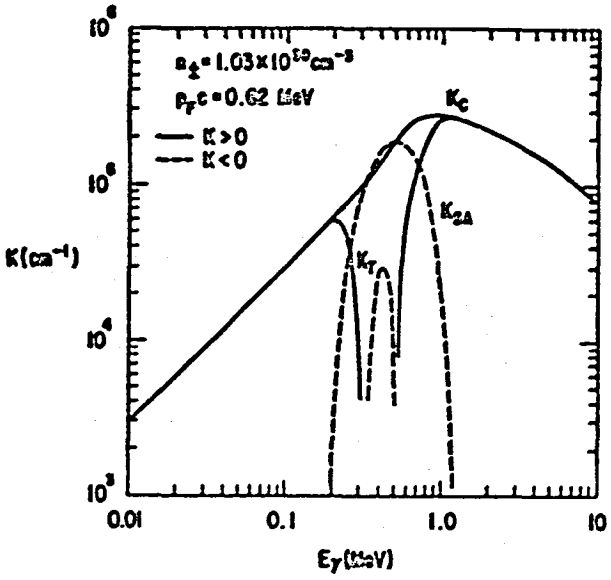

Figure 1. Absorption coefficients vs. photon energy in a degenerate positron-electron plasma.

Accurate calculation of K_{SA} and K_C for a degenerate positron-electron plasma have been carried out by RMJ[1]. In Fig. 1 we show their results for a pair density just above threshold. As can be seen, below the Fermi energy K_C indeed decreases rapidly with decreasing photon energy. By comparing the threshold density of $\sim 10^{30}\ \mathrm{cm}^{-3}$, obtained from the numerical calculations, with that given in Eq. (12), we see that $f = 0.6$, i.e. approximately 40% of the degenerate positrons and electrons cannot contribute to Compton scattering at ~0.5 MeV.

The threshold density for grasar action would be lower than $10^{30}\ \mathrm{cm}^{-3}$ if the Compton scattering cross section were less than πr_o^2. Indeed, in the presence of a strong magnetic field, at photon frequencies below the cyclotron frequency, ν_c, the Compton cross section is substantially reduced. But the observation[2] of cyclotron absorption features at 40-60 keV in many gamma-ray bursts suggests that for e^+-e^- annihilation photons $E \gtrsim 10\ h\nu_c$. Daugherty and Ventura[7] have shown that at such photon energies, the scattering cross section for photons directed parallel to the field is very nearly πr_o^2. Altogether, it seems that the density of pairs in a grasar source must exceed $10^{30}\ \mathrm{cm}^{-3}$.

THE CENTRAL ENERGY OF A GRASAR LINE

From their numerical calculations RMJ[1] found that the maximum of $-K_T$ is at a photon energy less than 0.5 MeV and from this they concluded that the central energy of a grasar line should also be at such a photon energy. There are two qualitative effects that cause this redshift. The first one can be seen from Figure 1. Here, for a degenerate pair plasma of density close to the grasar threshold, the maximum of $-K_{SA}$ occurs very close to 0.5 MeV. But because of the steep slope of K_C, the maximum of $-K_T$ is shifted to ~ 0.42

ORIGINAL PAGE IS
OF POOR QUALITY

MeV. This redshift, therefore, is a direct consequence of the effect of the degeneracy on Compton scattering and the high Fermi energy implied by the high threshold density.

The second effect is independent of the degeneracy. It is caused by either a high temperature ($kT \sim mc^2$) or a high density (Fermi energy $\sim mc^2$), both of which broaden and blueshift the emissivity[1]. Then from Eq. (10), division by E^2 moves the peak of $-K_{SA}$ to an energy <0.5 MeV. In the nondegenerate case, the peak of $-K_T$ essentially coincides with that of $-K_{SA}$, since K_C is not a strong function of photon energy. In the degenerate case, with the pair density much higher than the threshold density, the shape of K_C does not affect much the position of the maximum of $-K_T$.

Varma[8] proposed a grasar model based on degenerate pairs with Fermi energy $\ll mc^2$ for which the peak of $-K_{SA}$ would be very close to 0.511 MeV. However, Compton scattering was ignored in this model. If it were taken into account, then the relatively low pair density corresponding to this Fermi energy would imply that $K_{SA} + K_C > 0$ at all energies. Thus grasar action cannot occur in this model.

As pointed out in the Introduction, the observed annihilation lines in gamma-ray bursts are at ~0.43 MeV. If some of these lines are indeed from grasar sources, the implied gravitational redshift would be much smaller than that implied by spontaneous, nonamplified annihilation. The potential existence of grasar sources, therefore, allows gamma-ray bursts to be produced on neutron stars of smaller mass and larger radius than previously conjectured, or even objects other than neutron stars.

REFERENCES

1. R. Ramaty, J. M. McKinley and F. C. Jones, Ap. J. 256, 238 (1982).
2. E. P. Mazets, S. V. Golenetskii, R. L. Aptekar', Yu. A. Gur'yan, V. N. Il'inskii, Nature 290, 378 (1981).
3. B. J. Teegarden and T. L. Cline, Ap. J. 236, L67 (1980).
4. W. K. H. Schmidt, Nature 271, 525 (1978).
5. T. L. Cline et al., Ap. J. Lett. 255, L45 (1982).
6. R. Ramaty, R. E. Lingenfelter and R. W. Bussard, Astrophys. Space Sci. 75, 193 (1981).
7. J. K. Daugherty and J. Ventura, Phys. Rev. D 18, 1053 (1978).
8. C. M. Varma, Nature 267, 686 (1977).

END

DATE

FILMED

AUG 26 1983

LANGLEY RESEARCH CENTER
3 1176 00515 5180